ELSEVIER

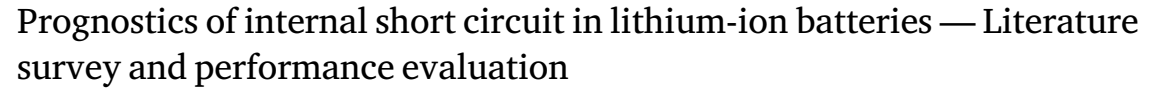
Contents lists available at ScienceDirect

Journal of Power Sources

journal homepage: www.elsevier.com/locate/jpowsour



Review article



Yongtao Yao ^{a, b, *}, Xinyu Du ^b, Shengbing Jiang ^b, Rasoul Salehi ^b, Erik Huemiller ^b, Weisong Shi ^a

- ^a University of Delaware, Newark, DE 19702, USA
- ^b General Motors, Warren, MI 48092, USA

HIGHLIGHTS

- Comprehensive survey of ISC diagnostic and prognostic in lithium-ion batteries.
- · Evaluates diagnostic accuracy of direct vs. indirect ISC detection methods.
- · Sensitivity analysis reveals parameter impact on short circuit estimation.
- · Benchmark comparison includes both lab tests and real-world EV data.
- · Discusses future directions for safe and scalable battery fault monitoring.

ARTICLE INFO

Keywords: Lithium-ion battery EV Diagnostics Prognostics Internal short circuit

ABSTRACT

Li-ion batteries may experience internal short circuits (ISCs), which can lead to increased energy usage, decreased efficiency, reduced capacity, and impaired performance. In severe cases, ISCs may cause thermal runaway, posing risks of fires or explosions. Therefore, diagnostics and prognostics (D&P) of ISCs are essential to electrical vehicle driving experience. Existing literature surveys on ISC either do not include the state-of-the-art D&P approaches after 2021 or do not provide qualitative and quantitative performance comparison, making it challenging to assess the respective strengths and limitations of different methods. This survey is conducted to fill this gap by examining over 30 D&P methods, including both physics-based models and data-driven techniques. A detailed analysis of these methods is provided, with their performance evaluated through sensitivity analysis and validation using actual test data. Our evaluation reveals that direct ISC diagnostic methods such as Cell Droop Rate exhibit significant estimation errors (approximately 80%–90%) in real vehicle data, highlighting the critical need for improved robustness and accuracy. Based on the evaluation, some key challenges in current ISC D&P are identified, and future research directions are proposed.

1. Introduction

The transition from fossil fuels to cleaner, renewable energy sources sparks a revolution in the automotive industry, leading to the widespread adoption of electric vehicles (EV). At the core of this transformation lies the lithium-ion (Li-ion) battery, which is considered the preferred power source for EVs due to its high energy density, long cycle life, and relative efficiency [1]. In recent years, the global market for EVs and Li-ion batteries has experienced exponential growth, representing a significant technological advancement that supports a sustainable future. The Global EV Outlook 2024 report by the International Energy Agency highlights that over 10 million electric vehicles are on the roads globally, with significant growth in charging infrastructure, advancements in battery technology, increasing investments, and supportive

policies aiming for EVs to represent 30% of the global vehicle fleet by 2035 [2]. Along with the remarkable benefits, Li-ion batteries present critical challenges, particularly the risk of thermal runaway. Thermal runaway is a self-sustaining, exothermic reaction that can be triggered by overcharging, mechanical abuse, design/manufacturing defect, or fault degradation [3,4]. The root cause is often a breakdown in the separator, allowing the electrodes to come into direct contact, namely internal short circuit (ISC). The subsequent uncontrolled reactions can be catastrophic, leading to intense heat generation, fire, or even explosions, which may cause significant damage to the battery, the vehicle, and its occupants. Furthermore, these incidents may result in not only financial losses but also environmental harm and damage to the reputation of original equipment manufacturers (OEM) [5]. Given

^{*} Corresponding author.

E-mail address: yongtao@udel.edu (Y. Yao).

these potential risks, the fault diagnostics and prognostics (D&P) of Li-ion batteries, especially ISC D&P, becomes a vital component in ensuring vehicle reliability. Effective D&P techniques, such as monitoring voltage and current fluctuations, impedance spectroscopy, thermal imaging, and sensor-based methods, are employed in both laboratory environments and real-world applications to detect, analyze, and mitigate issues [6]. Recent studies have further enhanced the understanding of battery thermal management systems. For example, Vashisht et al. experimentally evaluated heat-generating parameters, demonstrating the importance of incorporating dynamic resistance variations to improve thermal prediction accuracy [7]. Liu et al. employed a ternary hybrid nanofluid to optimize cooling performance in battery modules, achieving significant reductions in both maximum module temperature and internal temperature gradients [8]. Additionally, Yousefi et al. investigated the effectiveness of liquid immersion cooling using enhanced Al₂O₃ nanofluids for large-format prismatic battery packs, underscoring the critical role of optimized thermal control strategies in preventing thermal runaway incidents [9].

There exist some surveys offering valuable insights for mainstream ISC D&P methods, and categorizing them into offline and online approaches, parameter inconsistency-based methods, and model-based techniques [10,11]. These surveys are instrumental in advancing the understanding of ISC detection up to their publication time and have served as helpful resources for researchers in the field. However, there are some drawbacks to these surveys. Firstly, the existing surveys, published before 2021, do not include the latest developments. Additionally, there is no qualitative and quantitative comparison, making it difficult for readers to understand the status of the ISC D&P performance [12,13].

To solve these issues, we embark on a comprehensive examination and comparative analysis of the predominant methodologies employed in battery prognostics, including an in-depth discussion of their enabling conditions and performance. The root causes and modeling of ISC are explored followed by a survey of a variety of D&P approaches, ranging from electrochemical impedance spectroscopy to advanced artificial intelligence/machine learning (AI/ML) models [14–16]. These methodologies are meticulously classified to illustrate their underlying principles and operational frameworks. The landscape of battery D&P techniques is diverse and multifaceted. Our report classifies these methods into distinct categories based on their D&P principles, such as electrochemical modeling and analysis, physical or empirically modeling and analysis, and data-driven based modeling and analysis. Within each classification, we scrutinize the operational prerequisites and the contexts in which these methods are most effective. The comparison draws on a multitude of criteria, including sensitivity to battery conditions, adaptability to varying operational modes, and the capacity for early detection of potential failures [17]. A sensitivity analysis of selected D&P methods is also conducted. The robustness of these methods against perturbations in their operational parameters is evaluated, revealing their strengths and potential limitations. Furthermore, these methods have been subjected to rigorous evaluation on diverse datasets, encompassing both controlled experimental data and real-world operational data from electric vehicles [18]. The empirical assessments provide invaluable insights into the practicality and reliability of these techniques in actual use scenarios. The ultimate objective of our report is to distill complex D&P methodologies into accessible knowledge, thereby empowering the research community with the understanding necessary to deploy the most appropriate and effective tools for advancing battery reliability in EVs.

The rest of this report is organized as follows. Chapter 2 discusses the root causes and impacts of short faults. Chapter 3 systematically classifies and outlines the state-of-the-art D&P methods, providing insights into their operational principles and contexts. Following this, Chapter 4 offers a qualitative and quantitative comparison of these methods, analyzing their effectiveness across various scenarios and datasets to underscore their strengths and limitations. Chapter 5 describes the current challenges in ISC D&P related to data limitations, algorithmic challenges, and other technical hurdles, and then outlines future research directions informed by these challenges.

Table 1
Nomenclature, greek symbols, subscripts, and superscripts.

Symbol	Definition			
Q	Battery charge capacity (Ah)			
I	Current (A)			
V	Voltage (V)			
R	Resistance (Ω)			
C	Battery capacity (Ah)			
Δt	Time interval (s)			
dV/dQ	The derivative of battery voltage with respect to charge capacity			
dSOC	Differential State of Charge			
OCV	Open-circuit voltage (V)			
SOC	State of charge (%)			
ε	Estimation error (%)			
δ	Parameter variation coefficient			
a	Voltage decay slope			
k	SOC/OCV mapping coefficient			
g	Constant relating voltage to charge variation			
Subscripts and Superscripts				
j	Cell group index			
m	Module median cell			
S	Short-circuit related parameter			
usage	Parameter due to external usage			
bal	Parameter due to cell balancing			
0	Initial or nominal condition			
i, i + 1	Timestamps at intervals			

Table 2
List of acronyms and abbreviations.

Acronym Definition		
ISC	Internal Short Circuit	
D&P	Diagnostics and Prognostics	
OEM	Original Equipment Manufacturer	
LIB	Lithium-ion Battery	
ANN	Artificial Neural Network	
ESC	External Short Circuit	
OCV	Open Circuit Voltage	
SOC	State of Charge	
EV	Electric Vehicle	
ECM	Equivalent Circuit Model	
BMS	Battery Management System	
CNN	Convolutional Neural Network	
RNN	Recurrent Neural Network	
LSTM	Long Short-Term Memory	
RF	Random Forest	
SVM	Support Vector Machine	
EIS	Electrochemical Impedance Spectroscopy	
P2D	Pseudo-Two-Dimensional Model	
FEA	Finite Element Analysis	
NMC	Nickel Manganese Cobalt	
SEI	Solid Electrolyte Interphase	
FDR	Fault Detection Rate	
FAR	False Alarm Rate	

2. Understanding of internal short circuit

ISC is a common fault for lithium-ion batteries. This fault is caused by unintended electrical connections between the cathode and anode, resulting in the release of stored energy as heat internally. The fault may escalate into dangerous thermal events such as runaway reactions, fires, or explosions if the short resistance is small. Due to its frequency and potential severity, it is critical to understand ISCs, including why they occur, their impact on battery performance and reliability, and how to model them. To enhance clarity, Table 1 summarizes the key notations used throughout the manuscript, including Latin and Greek symbols, as well as subscripts and superscripts. Table 2 provides a comprehensive list of acronyms and abbreviations commonly referenced in this study.

2.1. Definition and causes

An ISC occurs when an unintended direct electrical connection forms between the positive and negative electrodes inside a battery, bypassing the separator. This short-circuits path allows a current to flow. When the path is large, heat is generated rapidly, which may cause the electrolyte to decompose, releasing gases and potentially leading to catastrophic failure called thermal runaway, i.e. fires or explosions [19-21]. This phenomenon is a significant concern in lithium-ion batteries due to their widespread use in various applications, including electric vehicles, portable electronics, and energy storage systems. ISC in lithium-ion batteries are categorized into soft short and hard short based on separator failure mechanisms observed under mechanical stress. Soft shorts occur due to localized separator tearing, allowing limited electrode contact and gradual energy dissipation, often undetectable by conventional voltage monitoring. Hard shorts result from large-scale structural collapse, causing extensive electrode bridging and rapid heat accumulation that triggers thermal runaway [22,23]. Soft shorts may evolve into hard shorts if dendrites fully penetrate the separator, emphasizing the dynamic nature of failure progression [24]. The causes of ISCs in lithium-ion batteries can be broadly categorized into internal and external factors. Internally, ISCs may occur due to manufacturing defects, dendrite/solidate electrolyte interphase (SEI) growth, chemical instability, electrode-tab electrical degradation, and ion conductivity reduction [25,26]. Manufacturing defects may include torn tabs, uneven electrode coating, misalignment of battery layers, or damaged/sliced separator [27]. Imperfections during welding or the presence of microscopic metal particles can also create pathways for electrical current that bypass the normal route. Over time during vehicle operation, degradation mechanisms such as SEI growth, lithium dendrite growth, or lithium plating can damage the separator, leading to an unintended electrical connection between the anode and cathode [28]. Additionally, mechanical failures, including torn tabs or other forms of structural degradation, may happen during the whole EV lifecycle, which compromise the integrity of the separator and contribute to ISC [29,30]. Electrode-tab degradation is another critical factor, where connections between electrodes and tabs degrade over time due to mechanical stress or corrosion, leading to an intermittent disconnection of some electrode. Frequent connection/disconnection is known to cause localized heating and uneven current distribution, which may eventually result in unintended current paths between electrodes (e.g., lithium dendrite), increasing the risk of ISC [31,32]. Reduction in ion conductivity within the electrolyte can also contribute to ISC. as factors such as improper electrolyte composition, contamination, or aging can reduce ion mobility, leading to uneven current distribution and localized heating and increase the likelihood of ISC [33,34]. ISCs can also be caused externally by mechanical damage such as impacts from accidents, where the casing and internal structure of batteries are compressed or punctured [35,36]. Such an event directly jeopardizes the physical barriers between electrodes, leading to shorts. The external pressure applied to the sides of the pouch cell during installation or operation sometimes causes the separator to recede or the internal structure to change, potentially leading to soft or hard ISC. External factors such as rapid temperature changes are known to induce material expansion or contraction, potentially compromising internal structures and leading to short circuits. Additionally, the incorporation of battery packs in complex electronic systems can expose them to electrical anomalies from other components, such as voltage spikes, which may precipitate internal shorts. The external and internal factors may occur simultaneously or alternatively, leading to the degradation towards ISC.

2.2. Impacts of internal short circuits

ISC can manifest as either a hard short or a soft short, each of which impacts the battery performance differently. Soft shorts involve

a pathway with relatively high resistance, resulting in a slow selfdischarge for the affected cell. Unlike hard shorts, soft shorts do not immediately lead to thermal runaway. However, the continuous selfdischarge causes the cell's OCV to drop below that of healthy cells. This voltage discrepancy is managed by the BMS balancing mechanisms to compensate such imbalance, leading to unnecessary energy consumption, reduced overall efficiency of the battery pack, and a decrease in the driving range of EVs [37]. Over time, the persistent self-discharge is observed to accelerate battery aging, reduce capacity, and degrade performance [38]. Long-term effects are associated with a decreased lifespan of the battery pack and the need for more frequent maintenance or replacements, thereby increasing long-term costs for the vehicle owner. Hard shorts involve a low-resistance path between the anode and cathode, leading to a substantial and rapid flow of current. This sudden surge of current can generate excessive heat, which causes thermal runaway—a self-sustaining exothermic reaction resulting in fires or explosions, posing serious risks to passengers and bystanders [39]. The rapid discharge and overheating associated with hard shorts are known to severely damage the battery cells, causing an immediate and permanent loss of capacity and lifespan [40]. This not only compromises the battery's ability to store and deliver energy efficiently but can also render the entire battery pack unusable, necessitating costly replacements or repairs. Another side effect is the environmental challenges of disposing damaged batteries, as they contain hazardous materials requiring proper recycling or disposal [41]. From the perspective of OEMs, both hard and soft shorts should be addressed. While hard shorts present immediate safety hazards with catastrophic potential, soft shorts lead to gradual degradation that can undermine consumer confidence and satisfaction [42]. The nature of soft shorts makes them harder to detect early and accurately, potentially allowing the degradation to progress unnoticed until significant performance loss occurs. Consequently, robust safety protocols and advanced monitoring systems are essential to detect and mitigate the risks associated with both types of ISCs, ensuring the reliability of EV batteries throughout their operational lifespan.

2.3. ISC modeling

Modeling ISCs in lithium-ion batteries plays an important role in understanding the underlying mechanisms, developing and validating D&P algorithms before practical implementation [43]. However, capturing the complex, rapid, and nonlinear nature of ISC events presents significant challenges [44]. Traditional equivalent circuit models are used as a foundational basis for simulating battery behavior but are limited in capturing the intricate dynamics of ISCs, such as localized heating, electrochemical degradation, and mechanical stress [45-47]. Therefore, more advanced modeling techniques have been developed to bridge this gap and offer deeper insights into ISC formation and progression. The Equivalent Circuit Model (ECM) is one of the fundamental approaches used to simulate the behavior of lithium-ion batteries, including the occurrence of ISCs. A combination of resistive and capacitive elements is used in ECM to represent the battery, providing a simplified yet effective means to understand and predict battery performance under various conditions. A typical static ECM model is presented in Fig. 1, specifically illustrating the representation of an ISC within a lithium-ion battery [48]. The resistance R_0 is used to represents the ohmic resistance, accounting for internal resistances. The model can be expanded by combining additional resistive and capacitive elements to capture the dynamic characteristics of the battery under different conditions. To capture ISC and cell balancing impacts, two additional branches are included in the model and arranged in parallel. The presence of an internal short circuit is represented by the resistor short resistance, causing a direct current flow through it. This path is found to bypass the normal battery load and create a parasitic current, leading to localized heating and potential damage, such as rapid capacity loss or thermal runaway [39]. While ECMs can

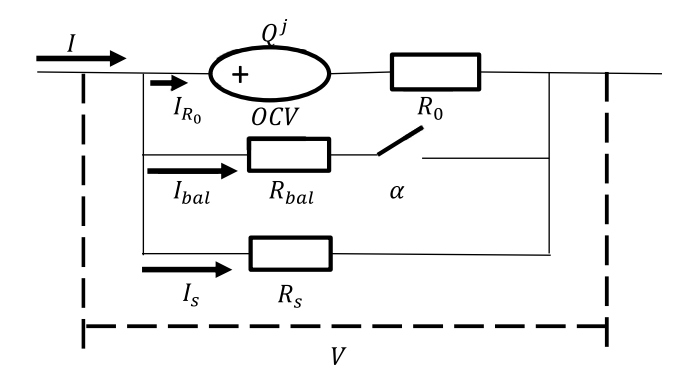


Fig. 1. Static ECM model for a cell with ISC and balancing circuit.

simulate certain battery behaviors, they are limited in describing the internal structure of the battery, such as localized phenomena like shorts between cell components, electrode porosity, and material degradation [49]. To address these limitations, the Pseudo-Two-Dimensional (P2D) model is introduced, which provides a more comprehensive approach by considering the internal electrochemical and physical processes within lithium-ion batteries. P2D model is shown in Fig. 2, an electrochemical model commonly used to understand the internal mechanisms of lithium-ion batteries. The P2D model is based on the concentrated solution theory and porous electrode theory, which describe how ions move through the electrolyte and interact with the electrode materials [50,51]. In the P2D model, the electrodes are represented as porous structures filled with active material particles, usually modeled as spheres of uniform size, increasing the specific surface area and enhancing electrochemical reactions [52]. The model simulates the movement of lithium ions through the electrolyte, considering concentration gradients and ion conductivity, which affect overall battery performance and response to ISC events. It describes the electrochemical reactions occurring at the electrode-electrolyte interface, and how ISC alters the local reaction environment, leading to further degradation. The model considers electron flow in the electrode and ion flow in the electrolyte, representing the charge transport mechanisms directly influenced by the presence of ISC. The P2D model calculates mass transfer within the battery, including lithium insertion/extraction in the electrode and diffusion in the electrolyte.

For ISC detection, the P2D model captures local heating and degradation effects caused by ISC but are often not accounted for in simpler models like ECM. This includes temperature rise near the short circuit, which accelerates the degradation. By observing electrochemical changes within the battery, such as altered lithium-ion transport and reaction kinetics, the P2D model can identify characteristics of ISC. These characteristics manifest as deviations in predicted voltage, current distribution, and thermal curves compared to a healthy battery. The model can dynamically simulate the development of ISC, aiding in predicting changes in faults over time and their impact on battery performance. This makes it useful for validating ISC detection algorithms that rely on identifying these electrochemical anomalies.

While ECM and P2D models provide valuable insights to the battery's electrical and electrochemical behaviors, they still have limitations in capturing the full complexity of ISC events, particularly those involving interactions between thermal, mechanical, and electrical phenomena. These models often overlook factors such as mechanical stress, electrode deformation, and temperature gradients that can significantly impact ISC initiation and progression. To address these gaps, multiphysics models are introduced, integrating multiple physical processes to provide a comprehensive analysis of ISC behavior. Yao et al. recently conducted detailed comparative analyses and simulations of high-power and high-energy lithium-ion batteries, highlighting the limitations of traditional pseudo-two-dimensional (P2D) modeling methods and the necessity of parameter adjustments for precise capacity predictions under high discharge rates [53].

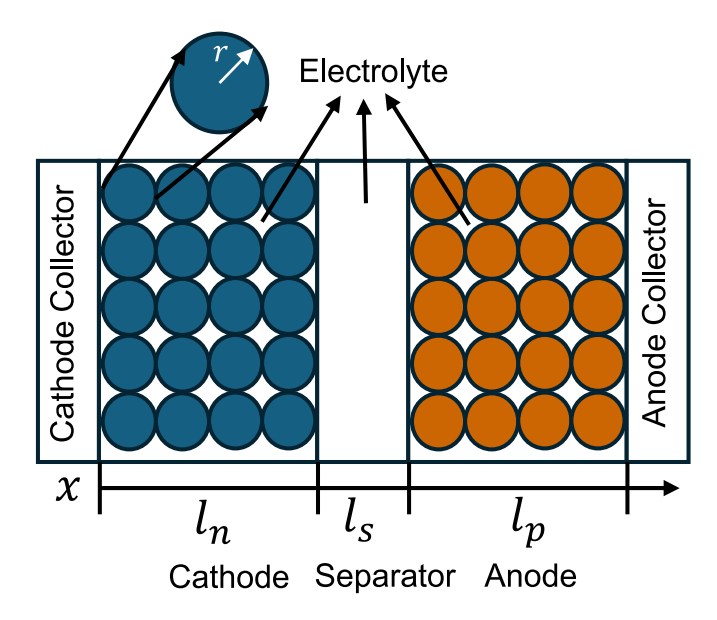


Fig. 2. Schematic representation of the P2D model for lithium-ion batteries. This model integrates multiple physical phenomena, including electrolyte-phase lithium transport, electrochemical reaction kinetics at the electrode-electrolyte interface, electronic and ionic conduction, and mass balance considerations across different battery components [52].

Multi-physics modeling has become a cornerstone for simulating ISC mechanisms in lithium-ion batteries, integrating thermal, mechanical, and electrochemical dynamics to capture complex failure modes [54]. Traditional ECMs and P2D frameworks often neglect the coupled effects of heterogeneous stress factors, such as external mechanical impacts and material fatigue, which are critical for ISC initiation. In contrast, multi-physics approaches explicitly resolve these interactions through coupled partial differential equations (PDEs) [44].

A. Thermal-Electrical Coupling. Localized joule heating from ISC current paths (> $10~{\rm A/cm^2}$) generates temperature gradients exceeding 50 °C/mm within cell layers. Finite element analysis (FEA) tools like COMSOL Multiphysics® implement energy conservation equations to simulate this behavior [55]. Experimental validations using infrared thermography have demonstrated that such models can predict thermal runaway thresholds with less than 10% error compared to empirical measurements for NMC cathodes [56]. For example, dynamic loading tests under mechanical abuse reveal that temperature spikes precede voltage drops by 8–15 s, providing a critical early warning window [57].

B. Mechanical Stress-Driven Failure. Electrode volume expansion in silicon-based anodes (up to 10% strain) and external crush loads (>5 kN) can induce separator puncture, a primary ISC trigger [58]. Notably, multi-field simulations reveal that separator rupture occurs when von Mises stress exceeds 120 MPa in commercial polyethylene separators, a threshold validated through in-situ mechanical compression experiments [59].

C. Electrical Anomaly Signatures. Coupled electro-thermal simulations identify characteristic ISC signatures, including voltage plateau shifts ($\Delta V < 50$ mV) during relaxation phases and transient impedance reductions (20%–40% drop within 10 ms post-ISC initiation) [60]. These findings align with differential voltage analysis (dQ/dV) studies showing that micro-shorts alter local current distribution, broadening voltage peaks by 15%–30% in early-stage ISC cases [15]. Field data from electric vehicle battery packs further confirm that cross-voltage correlation coefficients drop below 0.85 within 5 min of ISC onset, enabling real-time detection [61].

D. Stochastic Quantification. Stochastic modeling techniques, such as Monte Carlo simulations, address manufacturing variability by incorporating parameters like graphite anode particle size distributions and

separator porosity tolerances ($\pm 5\%$) [62]. The National Renewable Energy Laboratory (NREL) has further developed open-source toolkits that combine multi-physics models with experimental databases, achieving 90% accuracy in predicting ISC scenarios under diverse operating conditions [63].

2.4. Datasets for ISC D&P

The dataset with the ISC fault is crucial for advancing research on ISC D&P. In this section, the ISC related datasets are reviewed and compared.

2.4.1. Open-source datasets

Open-source datasets greatly facilitate battery research, particularly in estimating battery states such as State of Charge (SOC), Remaining Useful Life (RUL), and State of Health (SOH), along with degradation processes. For instance, the NASA Battery Dataset is used to provide valuable data on lithium-ion battery degradation under fixed chargedischarge life cycles, while the Randomized Battery Usage Dataset provides dynamic insights into SOC and SOH under real-world, nonstandard conditions [64,65]. Additionally, the Oxford Battery Degradation Dataset provides detailed battery health across its entire lifespan [66], and the Drive Cycle Battery Dataset contains SOC and RUL estimations during simulated automotive driving cycles [67]. The CALCE Battery Performance Dataset offers temperature-related data, crucial for designing robust EV battery systems [68]. However, none of these opensource datasets includes the data with ISC faults. Several proprietary datasets described in research papers are used to provide experimental data with ISC faults, offering valuable insights into the behavior of lithium-ion batteries under fault conditions. These datasets often involve custom-built or commercially available battery cells, along with detailed analysis of their electrochemical and material properties. For instance, a study inducing dynamic overcharge of lithium-ion batteries under different environmental conditions uses a single cylindrical lithium-ion cell, which were subjected to controlled overcharge and elevated temperature conditions to induce ISC [69]. The dataset includes signals such as voltage, temperature, and current, providing a detailed examination of how these parameters evolve during fault scenarios. The study on enhancing Li-ion battery safety by early detection of nascent internal shorts utilized a Sanyo 18650SA lithiumion battery, focusing on the self-discharge characteristics and thermal stability under various cycling conditions [70]. Real-world data from electric vehicle operations also plays a crucial role in understanding ISC behavior. For example, the National Big Data Alliance of New Energy Vehicles (NDANEV) dataset provides operational data collected from electric vehicles, tracking metrics like cell voltage, temperature, and current [71]. This large-scale dataset, containing data from up to 95 cells per vehicle, offers a comprehensive view of how ISC-related issues manifest in actual driving conditions. This dataset does not simulate ISC but captures real-world incidents, such as thermal runaway during charging. Electrochemical Impedance Spectroscopy (EIS) measurements are considered another powerful tool for detecting ISC. One study generated a dataset of over 840 EIS spectra from 5 NCM811 and 2 NCM523 commercial batteries, where ISC was simulated by paralleling resistances between 200 Ω and 10 Ω across the cells [72]. This dataset captured EIS data across a wide frequency range and different states of health (SOH), providing detailed information on how internal short circuits affect the impedance and electrochemical behavior of the cells.

2.4.2. Proprietary dataset

In addition to publicly available datasets, we obtained two proprietary datasets from an industry partner. These datasets provide experimental ISC data under controlled conditions. Coin Cell dataset is collected using small batteries with a capacity of 1Ahr. On-Vehicle Simulated ISC dataset contain high-frequency time-series signals, includes faulty cells from one real vehicle. Note that no thermocouples are used

during the experiments in our dataset. Therefore, surface temperature measurements and corresponding temperature plots are not available in this study. The following sections offer detailed descriptions of these datasets.

A. Coin Cell Dataset. The Coin Cell dataset contains laboratory cycling data that is collected from Lithium coin cell battery with separator damage faults. It includes three different profiles: static cycling, dynamic charge, and dynamic discharge profiles. C-rate is a measure of the rate at which a battery is charged or discharged relative to its nominal capacity; for instance, a 1C rate means that the discharge current will fully discharge the battery in one hour. For the static cycling profile, there are 300 cycles from 8 cells, with 4 cells exhibiting soft faults, sampled at 30 s (shown in Fig. 3(a), (b)). For the dynamic charge profile, there are 10 cycles from 8 cells, 4 of which are with soft short fault. The sampling rate is 1 Hz as shown in Fig. 3(c), (d). Similarly, there are 10 cycles from 8 cells with 4 faulty cells, sampled at 1 Hz for the dynamic discharge profile, as shown in Fig. 3(e), (f). This lab test dataset allows analyses of cell performance under different cycling conditions for both healthy and faulty cells. However, the severity of ISC fault, due to manually injected separator damage, is not quantitative measured. Consequently, while useful for developing and testing general ISC D&P algorithms, this dataset is inadequate for correlating the D&P results and the severity of ISC.

B. On-Vehicle Simulated ISC Dataset. This dataset is collected from real vehicles, but the ISC is simulated using additional resistance parallel to selected cells. Ground truth data for short circuit faults are very difficult to obtain in real-world operational scenarios, as such faults are both rare and potentially hazardous. To overcome this limitation, five resistors with known values are connected in parallel with five specific cell groups within the battery pack to simulate ISC conditions. Specifically, the dataset consists of samples collected once per second. These resistors, selected at five discrete levels within the 500–1500 Ω range, are used to simulate varying degrees of short circuit faults. As the ground truth is known, this dataset provides a clear and precise benchmark. As shown in Fig. 4, the figure presents nearly four months of data monitoring for eight cell groups (cells 104 to 111) from a vehicle. In Fig. 4(a), the current signal is mostly around zero. In fact, this data does not include driving information, but only a small amount of charging data, as indicated by the spikes in the figure. There is also some low-current charging data, while during the remaining time, the vehicle is at a stationary state but is constantly on, with the low-current discharging. Fig. 4(b) shows the voltage signals, where cell groups 104 -111 represent the cell group indices from the same module, with the faulty cell group (cell 108) is in red color. Its voltage starts lower than the other cells, but due to the effective compensation by the balancing mechanism in the vehicle, the voltage difference gradually decreases.

Due to the experimental nature of our dataset, inherent uncertainties from measurement instrumentation and environmental variations are expected. These uncertainties primarily arise from sensor measurement noise and calibration accuracy, potentially influencing voltage, current, and derived parameters like short-circuit resistance (R_s). Although specific uncertainty quantification details are unavailable, typical sensor uncertainties in battery experiments are usually within $\pm 1\%$ –2%, which should be considered when interpreting the presented results.

Simulation software such as MATLAB/Simulink, COMSOL Multiphysics, ANSYS, or GT-SUITE, used to build electro-thermal models, plays a vital role in understanding battery behavior. While this survey did not employ these simulation tools, numerous studies have leveraged them to investigate battery dynamics. For example, [53] constructed a pseudo-two-dimensional (P2D) model using COMSOL Multiphysics to simulate high-power and high-energy lithium-ion cell behaviors. Similarly, [8] utilized ANSYS Fluent to evaluate battery pack thermal management performance using nanofluid cooling, incorporating boundary conditions such as inlet velocity, cooling channel geometry, and ambient temperature. Additionally, [7] estimated internal

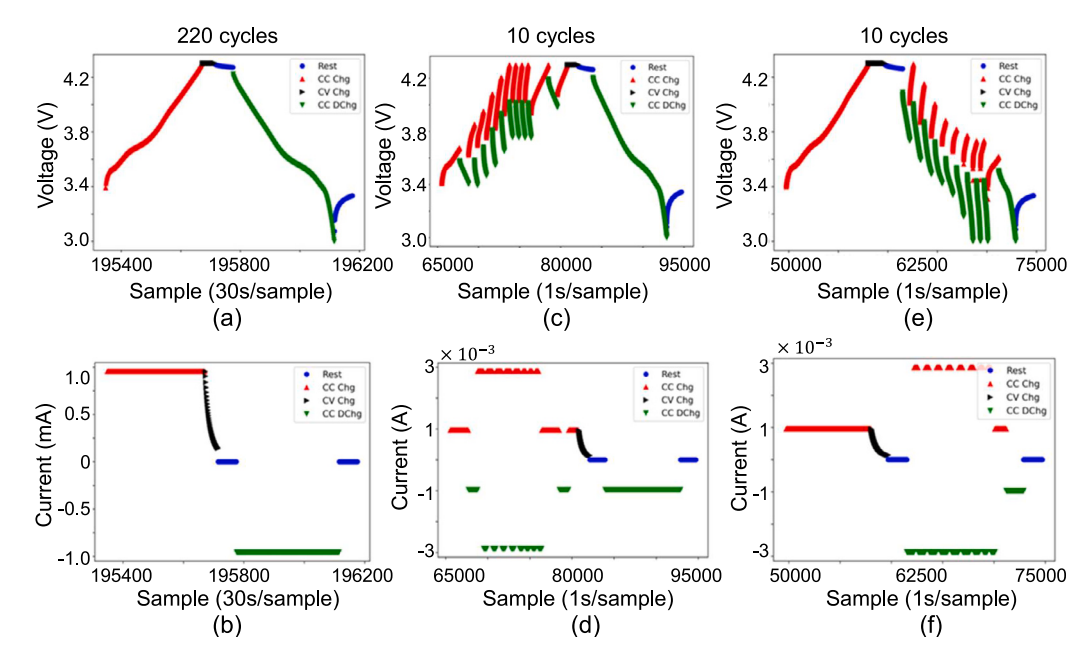


Fig. 3. Coin Cell Data Sample. (a) Voltage of one life cycle from stationary charging/discharging profile; (b) Current of one life cycle from stationary charging/discharging profile; (c) Voltage of one life cycle from dynamic charging/stationary discharging profile; (d) Current of one life cycle from dynamic charging/stationary discharging profile; (e) Voltage of one life cycle from stationary charging/dynamic discharging profile; (f) Current of one life cycle from stationary charging/dynamic discharging profile. All cells were charged using the standard Constant-Current followed by Constant-Voltage (CC-CV) protocol, where the current mode switched from CC to CV once the cell voltage reached the upper cutoff threshold. All discharging procedures were conducted using Constant-Current (CC) mode. In this plot, red-black-blue-green represent the states of CC Charge, Rest, and CC Discharge, respectively. Due to confidentiality constraints, we cannot provide the actual photograph of the experimental setup. (For interpretation of the references to color in this figure legend, the reader is referred to the web version of this article.)

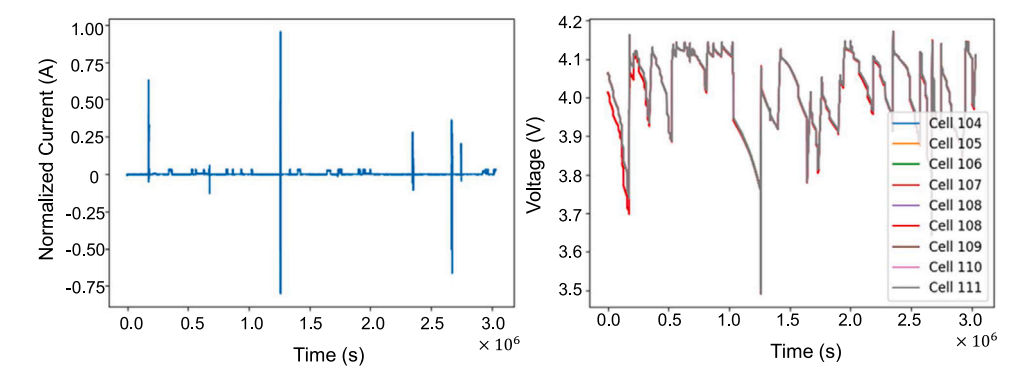


Fig. 4. On-Vehicle Simulated ISC Dataset. 10 samples/second for voltage, 1 sample/second for other signals. (a). Normalized current signal of the pack. (b). Voltage signals of 8 cells from one module.

resistance and entropy change parameters using inverse prediction techniques.

In such models, the equivalent circuit parameters R_1 , R_2 , and C are commonly used to represent battery internal characteristics: R_1 typically denotes the ohmic resistance of the cell, R_2 represents charge transfer resistance, and C is the double-layer capacitance. These parameters are usually obtained through EIS or model fitting to experimental data. While our dataset does not provide the necessary inputs to perform this level of simulation, we recognize the potential value of integrating modeling-based methods with ISC D&P pipelines, and consider it an important direction for future work.

The detailed technical specifications of the battery cells used in this study are subject to confidentiality agreements. While we are unable to disclose these specifics, the experimental methodology and overall study design remain transparent and sufficiently detailed to allow the community to understand and evaluate the validity and relevance of our experimental approach.

3. Battery D&P methods

In general, ISC D&P can be classified into electrical-based and nonelectrical-based approaches. Electrical-based methods typically analyze voltage, current, or other battery parameters, while non-electricalbased methods leverage other type of sensors, e.g. CO, CO2 and H2 gas sensors [73], temperature sensors [74] or pressure sensors [75]. The non-electrical methods generally detect ISCs when the battery is very close to failure. In contrast, electrical-based methods can provide early detection of ISCs, offering more opportunities to mitigate severe failures. Since the electrical signal sensors are also used for control purposes, electrical-based methods are more cost effective. Considering the benefit of electrical-based methods, in this work, the electricalbased ISC D&P methods are our focus, as shown in Fig. 5, which are described in two major subcategories: indirect D&P methods and direct D&P methods. For indirect ISC D&P methods, voltage fluctuations, SOC imbalances, temperature gradients, or impedance changes obtained by detecting electrochemical or thermal anomalies over time can be used to predict ISC. Direct short fault techniques, on the other hand, estimate

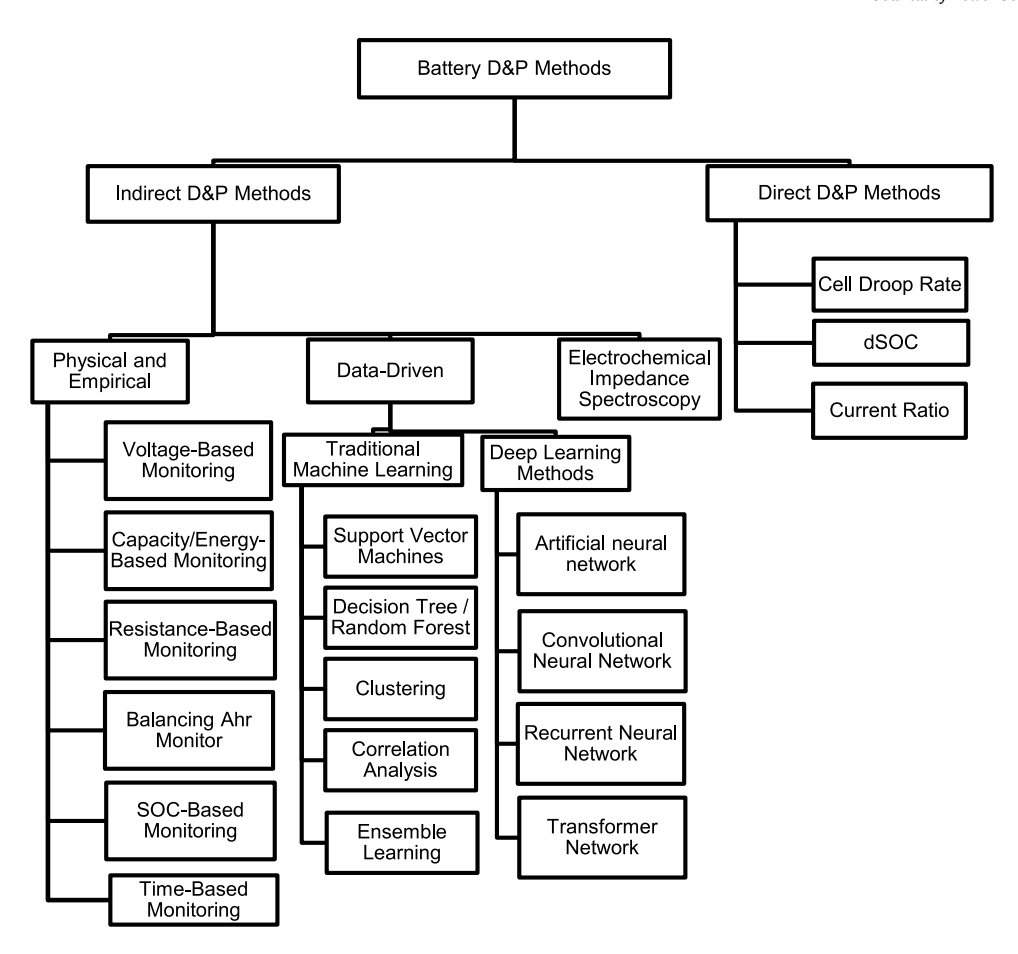


Fig. 5. Taxonomy of EV Battery D&P Methods.

short resistance directly, allowing not only for the detection of ISCs but also for a quantitative assessment of their severity.

3.1. Indirect D&P methods

3.1.1. Electrochemical impedance spectroscopy methods

Electrochemical Impedance Spectroscopy (EIS) has proven to be a critical tool for diagnosing ISC in lithium-ion batteries, particularly in identifying early-stage ISC faults. In one study, EIS combined with a deep neural network (DNN) achieved an ISC detection accuracy of 97.5% over the battery's full life cycle, with zero false positives. The system effectively detected changes in equivalent resistance from 200 Ω to 10Ω , demonstrating its applicability for real-time ISC detection [72]. Another study examined ISC detection under battery aging conditions using a frequency-domain P2D model to simulate impedance behavior. Experimental results from coin cell tests showed that ISC significantly altered low-frequency impedance, with diffusion coefficients increasing by 47% to 143% as the state of health (SOH) declined. This highlights the effectiveness of EIS in capturing early ISC faults by focusing on low-frequency components [76]. Some research, however, focuses on other fault types, such as electrolyte leakage [77], without directly addressing ISC. Additionally, EIS has contributed to general battery health assessments, such as refining state-of-charge (SOC) and state-of-health (SOH) estimations. EIS has been integrated with real-time systems for impedance estimation, providing precise measurements [78]. Moreover, studies have employed EIS to improve equivalent circuit models by incorporating elements like the solid electrolyte interface (SEI), which aids in SOC and SOH evaluation [79,80]. Despite these advancements, the high complexity and cost of EIS equipment remain challenges for onboard integration [78]. The measurement techniques for evaluating the state of power (SOP) of battery systems are also

critical for reliable D&P. Chen et al. proposed iterative power command searching methods to accurately measure battery SOP, addressing uncertainties related to current and voltage tolerance limits, which can impact battery performance D&P [81].

3.1.2. Physical and empirical D&P methods

Physical and empirical D&P methods utilize metrics such as voltage, current, SOC, and capacity to detect discrepancies between healthy and faulty cells. These discrepancies arise because the short fault may impact these measurements upon certain conditions. The primary advantage of indirect methods lies in their computational simplicity and sensitivity. Intuitively, an internal short may cause energy loss, longer charging times, lower rest voltage, higher charging capacity, or lower discharging capacity, changes in the OCV/SOC curve, changes in the electrode potential/capacity curve, and variations in internal resistance. However, the indirect methods cannot provide the short circuit resistance. Furthermore, for the soft short resistance that is greater than 100 Ohm, the impact of ISC for indirect D&P methods may be manifested by other noise factors or other failure modes.

Based on the characteristics of the methods, we list a series of indirect D&P methods below, some of which are referenced from the literature [82]. D&P methods proposed here are divided into several categories based on different battery parameters. These methods primarily use straightforward principles like dQ/dV analysis [83,84], time-based [85], voltage [17], current [86], capacity [87], and resistance estimations [88], with some methods derived from the 6-parameter ECM model [82]. Recent advancements also integrate machine learning techniques [83] and simplified electrochemical models [17] to enhance detection robustness and early-stage prognosis.

Table 3
Indirect ISC D&P methods

Categories	ISC D&P methods		
dQ/dV	1. dQdV_3.52, 2. dQdV_3.59, 3. dQdV_3.70, 13. CC_Chg_LinDQDV, 14.		
	CC_DChg_LinDQDV		
Time	5. CC_Chg_Time, 6. CV_Chg_Time, 7. CC_DChg_Time		
Voltage	8. Chg_Rest_linDV, 9. DChg_Rest_LinDV, 10. CC_Chg_LinDV, 11.		
	CC_Dchg_LinDV, 15. Rest_V_Drop, 17. Voltage level		
Current	12. CV_Chg_LinDI		
Capacity/Energy	4. Eng_Loss_Static, 16. DChg_Capacity, 22. Max_Chg_Cap, 26.		
	Eng_Loss_Dynamic		
Resistance	18. Static Charging Resistance, 19. Static Discharging Resistance, 20.		
	DV_a, 21. DV_RSC, 24. Delta_R, 25 Avg_DChg_R, 28. Pulse_R, 29.		
	6P_R0, 30. 6P_R1, 31. 6P_R2		
Capacitance	32. 6P_C1, 33. 6P_C2		
SOC/OCV Curve	23. SOC/OCV slope, 27. OCV_p, 34. 6P_OCV		

- dQ/dV methods, such as dQdV_3.52 and CC_Chg_LinDQDV, analyze charge–discharge characteristics, focusing on changes in the dQ/dV curve at specific voltage points.
- Time-based methods (e.g., CC_Chg_Time, CV_Chg_Time) track time changes during charge and discharge phases.
- Voltage methods (e.g., Chg_Rest_LinDV) assess voltage drop dynamics during different states.
- Current and capacity/energy methods estimate parameters like energy loss or capacity via integrals of voltage and current.
- Resistance methods (e.g., Static Charging Resistance, 6P_R0) estimate internal resistance under various conditions, including rest, charge, and discharge.
- Capacitance and SOC/OCV methods model capacitance and SOC dynamics, while electrode potential methods track potential differences across electrodes.

The detailed list of methods is shown in Table 3. For example, dQdV_3.52 refers to the value of the dQ/dV curve during the charging phase of the cell at 3.52 V. CC denotes constant current conditions, while Chg, DChg, and Rest represent charging, discharging, and resting states, respectively. LinDQDV describes the rate of change in the dQ/dV curve over time. Methods whose names start with 6P are based on parameters estimated from the 6-parameter ECM model. Static resistance is calculated by estimating the internal resistance during the transition from Rest to charge/discharge states, with OCV approximated from the final voltage in the Rest state. Q and Cap are obtained through time integration.

3.1.3. Data-driven based approaches

Data-driven based approaches can be categorized into two groups: Traditional machine learning approaches and Deep Learning approaches. Traditional machine learning is defined as an approach requiring structured data and feature engineering to select relevant features from raw data (e.g., voltage, current, or temperature signals) to train models for classification or regression tasks. In the context of ISC D&P, traditional ML techniques such as Support Vector Machines (SVMs) can be used to classify batteries as healthy or faulty based on preprocessed signals or to predict the probability of ISC occurrence. These methods are effective when a clear relationship exists between the input features and the target fault, but they typically rely heavily on manual feature extraction, which limits their ability to capture more complex patterns in the data. Deep Learning is a subset of machine learning that automatically learns features from raw data through multi-layer neural networks, such as Convolutional Neural Networks (CNNs). These networks can model complex, non-linear relationships in the data and are especially useful in handling time-series data, which is common in battery health monitoring. In ISC D&P, deep learning models can analyze large volumes of data from various sensors without the need for explicit feature engineering. They can detect intricate patterns related to early ISC development and provide realtime insights, making them particularly suited for fault detection in dynamic and noisy environments like electric vehicles.

Traditional Machine Learning Approaches

Machine learning methods are used to analyze large volumes of battery data to identify patterns and anomalies that may be too complex or subtle for traditional physics-based models to detect. Physics-based models rely on specific, well-understood principles, but may struggle to capture the full complexity of battery behavior under varying conditions, while machine learning models can adapt to a wide range of inputs and learn from historical data, allowing them to generalize and detect faults like ISCs early. Machine learning excels in environments where there is a large amount of real-world data, and its ability to handle noise and non-linear relationships makes it highly suitable for battery diagnostics. Unlike physics-based approaches, which may require precise modeling and assumptions, machine learning can uncover relationships between various signals (such as voltage, current and balancing Amphr) without needing a detailed understanding of the underlying physical processes. This makes it especially useful in cases where those processes are not fully understood or are too complex to model directly.

A. SVM method. SVM are supervised learning models that work by finding the optimal hyperplane that best separates data points into different classes. The algorithm maximizes the margin between the closest data points (support vectors) from each class to ensure robust classification, even in high-dimensional spaces [89,90]. In several studies, SVM is utilized for battery fault diagnostics, but not all directly address ISC faults. For instance, in [91,92], SVM is applied to diagnose connection faults and external short circuits (ESC), but ISC was not investigated. [82] explores ISC faults triggered by mechanical abuse, simulating ISC by dropping batteries onto hard surfaces. External short circuit resistances are employed to generate training data. Although SVM is mentioned as part of the study, SVM's detailed results are not reported, implying its performance was not superior. In [15], the authors simulate ISC faults by creating controlled external short circuits in series-connected 18,650 cells and evaluated multiple machine learning techniques, including SVM. Although SVM is tested, it achieves 89.65% accuracy in identifying ISC faults. The gradient boosting decision tree (GBDT) model outperforms it, achieving 99.4% accuracy.

B. Decision Tree/Random Forest (RF) method. A Decision Tree works by recursively splitting the data into subsets based on feature values, creating branches that lead to decisions or classifications at each node. The algorithm selects splits that maximize the separation of classes or reduce variability (for regression). RF is an ensemble learning method that builds multiple decision trees during training and combines their outputs to make more accurate predictions. It reduces overfitting and increases robustness by averaging the results of individual trees, each built on different subsets of the data [93]. RF algorithms are widely applied to diagnose ISC faults in lithiumion batteries. In [83], the authors utilize an RF classifier to extract features from voltage and current differences in the battery pack, detecting and localizing ISC faults with minimal sensors. Experiments conducted under constant current discharge and New European Driving Cycle (NEDC) conditions achieve a detection accuracy of 97.059%.

In [82], ISC conditions are emulated by connecting external short circuit resistors across the battery terminals. The RF classifier is trained on both healthy and ISC-affected battery data, achieving a fault detection accuracy of 98.45%. In [94], RF is used to classify battery states based on voltage and current signals. Training data is generated via multi-physics simulations covering different SOCs and short circuit resistances, achieving F1 scores greater than 0.93 in ISC detection. In [95], an RF classifier is employed to distinguish between normal and ISC conditions. The RF model outperforms Logistic Regression and Deep Learning in terms of accuracy across various operating conditions.

C. K-means clustering method. K-means clustering is an unsupervised learning algorithm that partitions data into clusters by minimizing the distance between data points and the centroid of each cluster. It iteratively updates cluster centroids and assigns points to the nearest centroid until convergence [96]. K-means clustering algorithm is also used in ISC fault diagnostics in batteries. In [97], the authors use real running data from a big data platform for electric vehicles from management systems serving more than 200,000 new energy vehicles. Experimental data are selected from the battery cell voltages of three electric vehicles, where one of them a normal vehicle, and two of them are vehicles suspected of having ISC faults. K-means clustering algorithm is used to cluster the battery cell voltages and select the center of the clusters as a representative cell to reduce false alarms due to the variations of the battery cells. With this algorithm, ISC faults in faulty vehicles are successfully detected, showing good diagnostic accuracy and false alarm reduction. In [98], the authors use data from seven vehicles with abnormal voltage fluctuations or thermal runaway faults and three normal vehicles, all of which used Li-ion batteries. The experimental data is obtained from a real electric vehicle big data platform. By extracting the standard deviation of the battery cell voltage and the improved Pearson correlation coefficient of each vehicle as features, the faulty battery cells are identified by a K-means clustering algorithm, and the degree of the faults was quantified based on the Euclidean distance. The experimental results show that the method successfully identifies the sudden voltage drop in the ISC fault detection of the battery, and the overall diagnostic accuracy is more than 98%.

D. Correlation Analysis Methods. Correlation Analysis measures the statistical relationship between two variables, quantifying how one variable changes in relation to another. It helps in detecting linear dependencies, with high correlation values indicating a strong relationship that can be useful for identifying patterns or anomalies in data [99]. In [62], the authors avoided the impact of battery individual inconsistency on fault diagnostics by extracting voltage correlations between voltage sensors instead of direct voltage measurements. In the paper, a method based on Independent Component Analysis (ICA) and Principal Component Analysis (PCA) is proposed to quickly diagnose ISC faults by parallel processing of high-dimensional non-Gaussian correlation coefficient signals in combination with cross-battery sensor topologies. In the experiments, different degrees of ISC faults are simulated by connecting various resistors in parallel to the battery pack, and the experimental results show that the method can accurately detect and localize ISC faults in a delay-free manner, while having lower fault detection delays and higher detection rates than traditional methods. For ISC faults, the Fault Detection Rate (FDR) of the proposed method is 97.5%, while its False Alarm Rate (FAR) has a maximum value of 0.21% for ISC fault detection. In [100], the authors further used ICA in combination with Voltage Correlation Coefficient (VCC) to detect ISC faults by extracting the VCC signals between neighboring cell voltage measurements. To simulate different levels of ISC faults, the experiment varies the internal resistance by connecting different resistors in parallel between the battery electrodes. The experimental results show that the method can maintain stable detection under different fault intensities and automatically set the detection threshold to ensure that the detection delay is kept at the lowest level and the faulty battery cells are accurately isolated. F. Ensemble Learning method. Ensemble

Learning combines multiple models (such as decision trees or neural networks) to improve prediction accuracy and reduce variance. By aggregating the strengths of diverse models, ensemble methods, such as bagging and boosting, provide more reliable and generalizable results than individual models [101,102].

In [103], an ensemble learning-based correlation coefficient method was proposed for diagnosing ISC and voltage sensor faults in EV battery packs. Ensemble learning was utilized by integrating the diagnostic results from multiple sub-models, each based on different window widths of the correlation coefficient signals, allowing for a more robust detection across various fault intensities. The approach incorporated Bayesian probability and Independent Component Analysis (ICA) to combine the fault probabilities from each sub-model into a global fault diagnostics, addressing the challenge of selecting an optimal window width for ISC fault detection. The method is validated using a six-cell battery pack, where ISC faults are simulated by connecting resistors (10 Ω and 25 Ω) in parallel with individual cells to create faults of different intensities. The experimental setup generates 12,500 samples. The results showed that the ensemble method is highly effective, detecting ISC faults immediately after their occurrence, with high precision even in the presence of weaker ISC faults. The proposed method demonstrates improved fault identification accuracy and reduced false positive rates compared to traditional single-scale methods, with a detection accuracy exceeding 98% for ISC faults. In ISC fault diagnostics and prognostics, traditional machine learning methods vary in effectiveness. SVMs tend to perform relatively poorly compared to models like Gradient Boosting Decision Trees GBDT and RF, which consistently achieve over 97% accuracy in ISC detection. RF is particularly effective at handling complex data and works well with minimal sensor input. K-means clustering is also beneficial, especially in reducing false alarms and detecting early-stage faults. However, correlation analysis offers real-time fault detection but requires more complex setups. Overall, ensemble learning methods, which combine multiple models, provide more robust ISC detection and are a stronger choice.

Deep Learning Methods

Deep learning techniques have been applied in growing applications in the D&P of ISC for EV batteries, offering significant advancements in reliability. One of the key advantages of deep neural networks (DNNs) is their ability to capture long-term dependencies, which is crucial for the accurate detection of battery faults over extended periods. In [104], Jia et al. demonstrate a CNN-based framework for estimating shortcircuit resistance Rs from real battery data. They generated a large dataset (649,000 samples) from cycling tests with external short circuits and constructed a CNN architecture consisting of normalization, five convolutional layers, dropout, and fully connected dense layers. The inputs to their model included sequences of: Current, Voltage, charging capacity, charging energy, Total charging capacity, and Total charging energy, sampled at 1 Hz over 120-second intervals. Their CNN model achieved an average relative absolute error of 6.75% \pm 2.8%, and they thoroughly analyzed performance using regression plots, error histograms, and parametric design studies. This work underscores the viability of deep learning for direct resistance estimation.

A. Artificial neural network (ANN) based method. ANN serves as a fundamental architecture in deep learning, particularly well-suited for classification and regression tasks due to their ability to fully propagate information across densely connected layers. In the context of lithiumion battery diagnostics, ANN-based models demonstrate significant promise [105]. In [82], a fully connected network is used, and the ISC case is simulated using an external short-circuit resistor, and the training dataset consists of data from both healthy and faulty batteries with external short-circuit resistance. The training dataset consists of data from healthy batteries and faulty batteries with external short-circuit resistance, and several features such as SOC, voltage, and energy loss were extracted by recording the charging and discharging voltages and currents of the batteries. Finally, ISC faults are classified by models such as RF and ANN, and ANN classification accuracy reaches 97.97%

normal in normal and 100% fault in fault accuracy. In [106], does not directly involve ISC faults, but mainly discusses external short circuit (ESC) faults in electric vehicle Li-ion battery packs, utilizing voltage information for Prediction. The experimental design includes charging and discharging multiple battery packs and introducing a single cell ESC fault to collect current and voltage data. The method achieves high prediction accuracy (maximum error of 4.8% under charging conditions).

B. Convolutional Neural Network (CNN) based method. CNN is a deep learning model widely used in the fields of image processing and computer vision. Convolutional layer is the core layer of CNN and is used to recognize local features in an image. The convolutional layer slides over the input data through filters to extract convolutional neural network mimics the way the human brain processes images through the above hierarchical structure, starting from local features, extracting and integrating information layer by layer, and finally realizing the overall understanding and classification of images. This hierarchical structure allows CNNs to perform well in tasks such as image recognition and classification, and to have high computational efficiency and accuracy [107]. Progress has been made in ISC fault diagnostics of lithium-ion batteries using CNN methods. Seo et al. propose a CNNbased ISC detection method by constructing an equivalent circuit model of the battery through MATLAB/Simulink to simulate ISC faults with different degrees of severity, and preprocessing the terminal voltage data to remove the constant-current-related interference, and finally achieved a fault classification accuracy of 96.0% [108]. Goh et al. evaluate the ISC faults of parallel-connected batteries by constructing an electrochemical-thermal coupling model and using a CNN combined with the battery surface temperature distribution and verify the robustness of the method by employing the simulated data and training it with noisy inputs [109]. Seo et al. also uses the RC modeling method in MATLAB/Simulink to evaluate the ISC faults of parallel-connected batteries, and the method is validated by using simulated data and training with noise input. RC model in Simulink for ISC fault simulation and classified ISC faults with different resistance values by CNN and finally achieved 82.3% classification accuracy [110]. On the other hand, although Goh et al. propose a CNN-based battery fault detection method, their research direction is mainly focused on faults caused by mechanical damage rather than ISC fault detection [111,112].

C. Recurrent Neural Network (RNN) based method. RNN is a neural network model capable of processing variable-length sequence data, which is unique in having a temporal feedback mechanism. Unlike traditional feed-forward neural networks, RNNs consider the output of the previous time step when processing the input of each time step, which enables RNNs to model the contextual information in the sequence. RNNs process variable-length sequence data by updating hidden states at each time step, using the current input and the previous hidden state to compute the next. The hidden states capture temporal dependencies, making RNNs well-suited for tasks like natural language processing (NLP) and time series prediction [113]. However, traditional RNNs face issues like vanishing/exploding gradients, which are mitigated by advanced variants like Long Short-Term Memory (LSTM) and Gated Recurrent Units (GRU) through gating mechanisms that better handle long-term dependencies [114]. In [115], LSTM combined with a battery physical model is used to indirectly diagnose thermal runaway faults caused by ISC by predicting the surface and internal temperatures of the battery. The experimental data is obtained from NASA's battery charge/discharge dataset, and the experiments are set at different ambient temperatures (24 °C, 4 °C, and 43 °C), and the results show that the method is effective in predicting changes in battery temperature, and thus in detecting potential thermal runaway failures. Although this study focuses on thermal runaway, the cause of the failure is closely related to ISC. And in [110], the electrochemical-thermal-internal short circuit coupling model is directly combined with an LSTM model, based on battery current, voltage, temperature and SOC parameters to detect and categorize the internal short-circuit faults of batteries.

The study simulates and generates 1380 sets of battery internal short-circuit datasets, and the model's diagnostic accuracy reaches 88.41% and 92.03% in charging and discharging states, which can effectively determine the severity of internal short-circuits and give appropriate warnings. All the above studies effectively diagnose ISC faults using LSTM models, but the former focuses on the indirect detection of thermal faults, while the latter is more focused on the direct detection of ISCs.

D. Transformer based method. The core principle of transformer is based on the self-attention mechanism, which can efficiently capture long-distance features by calculating the dependencies between different positions in the input sequence and dynamically assigning weights. Different from traditional sequence models (e.g., RNN, LSTM), transformer has parallel computing capability, which can significantly improve the computational efficiency and the ability to handle long time sequences [116]. The transformer method is applied to the diagnostics of ISC faults in battery packs. In [117], a reconstruction model combining transformer and LSTM is proposed for ISC detection of battery voltage data. The time series features are extracted by a sequence encoder, and the decoder optimizes the reconstruction process using an attention mechanism and detects ISC by residual analysis with actual voltage data. The experimental data includes voltage data of 20 battery cells under different driving conditions, and ISC faults with 1 Ω , 5 Ω and 10 Ω resistance values are simulated. The results show that the model exhibits better accuracy and noise suppression in detecting minor ISC faults. On the other hand, in [118], a cycle segmentation-based transformer model is proposed for simultaneously extracting time-space and cycle information for ISC detection. The length of the sliding window is adaptively adjusted by the period analysis module to effectively extract the period features in the time series. The experimental data include the voltage data of 60 seriesparallel Li-ion battery packs under three operating conditions, and the ISC faults of 1 Ω , 3 Ω , and 5 Ω are simulated, and the test results show that the F1 scores of this model under different ISC severities are improved by 24.2% compared with other methods. Both studies show that the Transformer method is highly robust and versatile in the early detection and accurate diagnostics of battery ISC faults. In the current landscape of DNN methods applied to ISC diagnostics and prognostics in lithium-ion batteries, ANN has demonstrated strong performance, particularly in fault classification tasks, achieving high accuracy in detecting ISC faults. This is partly because many related studies have used small datasets, typically involving only one or a few batteries, and focus on relatively simple classification tasks without requiring fault quantification, which naturally leads to higher accuracy. However, these methods may need validation on larger and more diverse datasets to ensure robustness. While ANN's reliance on densely connected layers can sometimes limit its ability to capture complex temporal dependencies, CNNs are highly efficient for processing structured data and are effective when ISC faults exhibit spatial or local features. Nonetheless, CNNs may not be ideal for analyzing long-term sequences. RNNs, particularly LSTM variants, excel at modeling temporal dependencies, making them well-suited for ISC fault detection over time, though they may face computational challenges. Transformer-based models, which use self-attention mechanisms, provide excellent scalability and accuracy for handling long sequences, showing promise for early ISC fault detection.

3.2. Direct short fault D&P techniques

Direct ISC D&P techniques are specifically designed to estimate short resistance directly, providing a clear indication of the severity of such incidents. These methods' strength lies in their capacity to offer an intuitive and direct gauge of a short fault's impact. However, accurately and reliably estimating variables like short resistance is challenging due to their sensitivity to impact factors, which makes the precise quantification of short resistance a complicated task. Direct short fault

D&P is normally based on the ECM modeling shown in Fig. 1, which can be summarized in the following equation,

$$Q^{j}(t_{i+1}) - Q^{j}(t_{i}) = \int_{t_{i}}^{t_{i+1}} I dt - \int_{t_{i}}^{t_{i+1}} I_{cb}^{j} dt - \int_{t_{i}}^{t_{i+1}} V^{j} dt \times \frac{1}{R^{j}}.$$
 (1)

This equation describes the change in the cell's charge between two timestamps, t_i and t_{i+1} , where j represents the cell group index. The charge variation, $Q^j\left(t_{i+1}\right) - Q^j\left(t_i\right)$, can be expressed as the sum of three integral terms. The first term, $\int_{t_i}^{t_{i+1}} Idt$, represents the total current drawn from the battery during the time interval, as measured by the current sensor. The second term, $-\int_{t_i}^{t_{i+1}} I_{cb}^j dt$ accounts for the cell balancing current, which is obtained from the corresponding cell balancing signal. The third term, $-\int_{t_i}^{t_{i+1}} V^j dt \times 1/R_s^j$, represents the short-circuit current, where V^j is the cell voltage measured by the voltage sensor, and short resistance is the internal resistance of the cell. By accurately measuring the charge capacity difference, $Q^j\left(t_{i+1}\right) - Q^j\left(t_i\right)$, and knowing the values of the current, cell balancing current, and cell voltage, it becomes possible to estimate the short resistance of the battery cell. Simplifying this basic form of Eq. (1) using different constraints, the Cell Droop Rate method and dSOC method can be derived

A. Cell Droop Rate [119]. This method estimates short resistance using data during the rest phase, when the external current is zero (I=0) and cell balancing is neglected $(I_{cb}^{j}=0)$. The charge capacity difference, $Q^{j}(t_{i+1})-Q^{j}(t_{i})=\Delta Q^{j}$, the SOC change, and the cell capacity are related as shown in Eq. (2):

$$\Delta O^j = \Delta SOC^j * C. \tag{2}$$

Thus, the SOC change is proportional to the open-circuit voltage (OCV) change, $\Delta OCV^j = OCV^j - OCV_0$, with a factor k ($k = dSOC^j/dOCV^j$):

$$\Delta SOC^{j} = k * \Delta OCV^{j}. \tag{3}$$

In addition, ΔQ^j can be calculated by integrating the current, where the current is equal to V^j/R_s^j ,

$$\Delta Q^{j} = -\int_{t_{s}}^{t_{i+1}} V^{j} dt * 1/R_{s}^{j}. \tag{4}$$

The voltage integral, $\int_{t_i}^{t_{i+1}} V^j dt$, can be replaced by $\bar{V}^j * \Delta t$, where \bar{V}^j is the average value of the cell voltage. By relating the OCV change to the average cell voltage and the short resistance, an equation is derived that expresses the cell voltage as a function of time, the short resistance, and the initial OCV:

$$OCV^{j} = \left(-\overline{V^{j}} * \Delta t/R_{s}^{j}\right)/(C * k) + OCV_{0}.$$
(5)

Refer to Fig. 1, $-I_{R0} = I_s$ due to I = 0, where I_{R0} denotes the current flowing through resistor R_0 , and I_s denotes the current flowing through resistor R_s . Based on Fig. 1, Eq. (6) is obtained:

$$\left(OCV^{j} - V^{j}\right)/R_{0} = V^{j}/R_{s}^{j}.\tag{6}$$

Eq. (6) is transformed to give the following equation:

$$OCV^{j} = V^{j}/R_{s}^{j} * R_{0} + V^{j}.$$
 (7)

From Eq. (5) and Eq. (7), Eq. (8) can be obtained:

$$V^{j} = -\overline{V^{j}}/(R_{o}^{j} * C * k) * \Delta t + (OCV_{0} - R_{0}/R_{o}^{j} * V^{j}).$$
 (8)

Recursive least squares (RLS) method is used to estimate the internal resistance, R_s^j , from the cell voltage measurements over time.

B. dSOC [120]. The short resistance is not directly estimated by dSOC in production. Instead, dSOC is used as indicators to flag potential faults. However, based on engineering feedback, dSOC can be used to estimate short resistance for further diagnostic purposes. It assumes that the cell capacity (C) is constant and known, and the cell balancing current is negligible ($I_{cb}^{j}=0$). The charge capacity difference, ΔQ^{j} , is related to the SOC change, ΔSOC^{j} , and the cell capacity, $\Delta Q^{j}=\Delta SOC^{j}*C$. For the median cell in the module, the battery charge

 (ΔQ^m) difference is assumed to be solely due to the external current (I), as its short resistance is considered infinite. Thus, ΔQ^m satisfies the following two equations:

$$\Delta O^m = \Delta SOC^m * C, \tag{9}$$

$$\Delta Q^m = \int_{t_i}^{t_{i+1}} I dt. \tag{10}$$

By comparing the charge capacity difference of the cell of interest to the median cell to remove the usage impact, the short resistance can be estimated using the average cell voltage, the time interval, and the difference between the SOC changes (i.e., dSOC):

$$R_{s}^{j} = \overline{V^{j}} * \Delta t / \left(\Delta SOC^{m} * C - \Delta SOC^{j} * C \right). \tag{11}$$

Let $(\Delta SOC^m - \Delta SOC^j)/\Delta t$ be denoted as m_{sc} ; then Eq. (11) can be transformed into the following Eq. (12):

$$R_c^j = \overline{V^j} / \left(m_{sc} * C \right) \tag{12}$$

C. Current Ratio. Under a constant current discharge scenario, the differential voltage (dV) can be described as the change in open-circuit voltage (dOCV) which is directly proportional to the current (I) multiplied by a constant g, and the differential time (dt). This change can also be expressed in terms of the differential charge (dQ), leading to the equation $dV \approx dOCV = g \cdot I \cdot dt = g \cdot dQ$. For any given cell within a battery, the change in charge dQ and the consequent change in voltage dV can be broken down into three components: the change due to short circuiting dQ_s and dV_s , the change due to usage dQ_{usage} and dV_{usage} , and the change due to cell balancing dQ_{bal} and dV_{bal} . Here, usage refers to the changes brought by the external load consumption. These relationships are encapsulated in the equation:

$$dV = dV_s + dV_{usage} + dV_{bal}, (13)$$

where the right-hand side of the equation can be expressed as below:

$$dV_s + dV_{usage} + dV_{bal} = g \cdot (I_s + I_{usage} + I_{bal}) \cdot dt. \tag{14}$$

For a median cell, which does not experience shorting and thus no dV_s , the equation is simplified to:

$$dV^m = dV_{usage}^m + dV_{bal}^m (15)$$

The right-hand side of the Eq. (15) can be expressed as below:

$$dV_{usage}^{m} + dV_{bal}^{m} = g \cdot \left(I_{usage}^{m} + I_{bal}^{m}\right) \cdot dt \tag{16}$$

Subtracting Eq. (16) from Eq. (14) we derive the expression for the change in voltage due to short, considering the cell balancing and the usage with a correction factor (Δ_C):

$$dV_s + d2V_{bal} + dV_{usage} \cdot \Delta_C = g \cdot \left(I_s + I_{bal}(\text{time avg}) + I_{usage} \cdot \Delta_C\right) \cdot dt \quad (17)$$

where $d2V_{bal}=dV_{bal}-dV_{bal}^m$, and the left side of the equation can be expressed as $dV-dV^m$, denoted as d2V. In the case where the balancing current I_{bal} is zero and there is no correction factor Δ_C applied, the change in voltage due to short d2V divided by the short current I_s is equal to the differential voltage over current dV/I. This ratio is then used to determine the internal resistance associated with the short resistance, following the relation $R_s = V/I_s$. The comparison of various methods for estimating short resistance in lithium-ion batteries is summarized in Table 4. The table outlines each method's advantages and limitations, providing a comparative analysis crucial for researchers and practitioners in the field. The dSOC method is less impacted by capacity changes, yet it does not account for cell balancing and is similarly affected by k. The Cell Droop Rate shares these cons but is noted for minimal capacity impact. This comparative analysis aids in discerning the suitability of each method for different D&P scenarios.

Table 4
Comparison of different methods for short resistance estimation.

Method	Pros	Cons
dSOC	Less impact on usage.	Impacted by k , balance, and capacity.
Cell Droop Rate	Less impact on capacity.	Assume no usage. Impacted by k , measurement error, and balance.
Current Ratio	Less impact due to capacity and k .	Impacted by measurement error.

3.3. Research gaps

Our investigation into direct and indirect D&P methods reveals several gaps. Direct D&P methods are relatively scarce, and while machine learning and deep learning have been applied to ISC D&P, they are primarily used for classification tasks, such as categorizing the severity of faults, rather than directly estimating R_s . Despite achieving high accuracy, these approaches rely on relatively simple and limited datasets, with some experiments based on a single cell, raising concerns about their scalability to larger datasets. Furthermore, while direct D&P methods can estimate short resistance, short resistance is highly sensitive to factors like capacity, necessitating more robust methods to ensure accurate and stable estimations across varying conditions.

4. Performance evaluation and discussion

We introduce the relevant datasets in Section 2 and ISC D&P approaches in Section 3. Based on these datasets, we evaluate some D&P methods. It is important to note that not every D&P method can be applied to all datasets. Different types of evaluations are necessary to account for the unique characteristics of each dataset, including sensitivity analysis and applicability of ISC D&P methods. In this section, we focus on evaluating the sensitivity of several direct D&P methods, aiming to better understand their performance, advantages, and limitations. Indirect D&P methods are not involved in sensitivity analysis because they do not directly provide quantitative estimates of short resistance; their results are qualitative in nature, making them unsuitable for sensitivity analysis. Sensitivity evaluation allows us to determine how effectively each ISC D&P method responds to earlystage faults, especially in scenarios where subtle anomalies are difficult to detect. This process is essential for determining the appropriate conditions under which these indicators can be applied. There are three main types of data used for evaluation: simulation data, lab data, and real vehicle data. While we acknowledge the value of simulation data, it is not included in the primary evaluation within this survey. The simulated healthy cells' voltage showing highly consistent electrical signals. This makes faulty cell identification straightforward, and the main purpose of using simulation data is to validate the methods' correctness. Therefore, we exclude it from this section's evaluation. Due to the structure of this project, which is divided into three parts, we present initial results here using two selected datasets: the Coin Cell dataset for performance evaluation and discussion of the lab dataset, and the On-Vehicle Simulated ISC dataset for real vehicle data, containing faulty cells with known ground truth.

4.1. Sensitivity analysis

ISC D&P methods are chosen for their responsiveness to internal battery perturbations that signal short circuits. These methods are based on electrochemical principles and display notable changes during ISC-related internal reactions, making them feasible for real-time D&P applications. Sensitivity analysis is crucial for evaluating how factors such as capacity and SOC influence the accuracy and reliability of short resistance measurements. The relative error is used as a measure in the sensitivity analysis, as shown in Eq. (18),

$$\varepsilon = \left| \left(R_s - \widehat{R}_s \right) / R_s \right| * 100\%, \tag{18}$$

where (\widehat{R}_s) represents the estimated value of the true value R_s . Note that the indirect D&P methods (e.g., voltage slope and capacity change)

primarily serve as qualitative indicators for ISC detection, making them unsuitable for direct sensitivity analysis. Accurate sensitivity assessment requires quantitative ISC characterization methods (such as short resistance estimation), which directly link subtle changes in parameters to specific variations in R_s . Therefore, in this study, sensitivity analysis is focused solely on the direct D&P methods.

4.1.1. Sensitivity analysis of the cell droop rate method

The rate of voltage decay during the rest period (I=0) and cell balancing is neglected ($I_{cb}=0$) are use in the Cell Droop Rate method. In this approach, the slope of the voltage over time, denoted as a (a<0), is calculated to determine the short resistance. The estimated short resistance is derived using Eq. (19):

$$R_{s} = -\overline{V^{J}}/(a*C*k),\tag{19}$$

where $\overline{V^J}$ represents the average voltage of a cell, C is the battery capacity, and k is the SOC/OCV mapping coefficient. Both C and k are assumed to be known and constant. However, inaccuracies in these values can result in significant estimation errors.

A. Influence of k on R_s Estimation.

Assuming that the actual SOC/OCV mapping coefficient of a cell is k, but using $k * \delta$ in the R_s estimation process, this introduces the computational error expressed in Eq. (20):

$$\varepsilon = \left| \frac{-\overline{V^J}/(a*C*k) + \overline{V^J}/(a*C*k*\delta)}{-\overline{V^J}/(a*C*k)} \right| * 100\%, \tag{20}$$

It can be simplified to the following equation:

$$\varepsilon = |(\delta - 1)/\delta| * 100\%. \tag{21}$$

For example, assuming the true value of k is 1.15, but an approximate value of 0.5 ($\delta = 0.4347$) is used in the calculation, this will result in an estimated error of 130%.

B. Influence of C on R_s Estimation.

Assuming that a cell's actual capacity is C, but using $\delta * C$ in the R_s estimation process, this introduces the computational error expressed in Eq. (22):

$$\varepsilon = \left| \frac{-\overline{V^J}/(a * C * k) + \overline{V^J}/(a * C * \delta * k)}{-\overline{V^J}/(a * C * k)} \right| * 100\%, \tag{22}$$

It can be simplified to the following equation:

$$\varepsilon = |(\delta - 1)/\delta| * 100\%. \tag{23}$$

For example, assuming the true value of the cell capacity is 297 Amphr, but an approximate value of 300 Amphr ($\delta = 1.01$) is used in the calculation, this will result in an estimated error of 1.0%.

4.1.2. Sensitivity analysis of the dSOC method

For dSOC method, it is assumed that the battery capacity is constant and the known, and the cell balancing current is negligible ($I_{cb}=0$). This method estimates short resistance by measuring the SOC difference (denoted as ΔSOC) between the module median and a specific cell group over time, calculated as $dSOC=\left(\Delta SOC^m-\Delta SOC^j\right)/\Delta t$. The short resistance is then given by Eq. (24).

$$R_{\rm s} = \overline{V^j}/(dSOC * C) \tag{24}$$

where $\overline{V^j}$ is the average voltage of a cell. Unlike other methods, this approach assumes that SOC can be directly measured without

converting OCV using the SOC/OCV mapping coefficient (k). However, inaccuracies in C can lead to significant errors in the estimated R_s . When capacity decreases, the discharge accelerates, causing a change in the measured dSOC, denoted as dSOC'. Assuming the battery is discharging at a constant current I_s , with a short current I_s , and that the module median capacity ($C_m = C_0$), the required true dSOC for R_s estimation is calculated as:

$$dSOC = \frac{\int I dt}{C_m * \Delta t} - \frac{\int (I + I_s) dt}{C_0 * \Delta t}.$$
 (25)

However, the measured dSOC' is calculated as the following equation:

$$dSOC' = \frac{\int I dt}{C_m * \Delta t} - \frac{\int (I + I_{\delta}) dt}{\delta * C_0 * \Delta t}.$$
 (26)

The ratio $\frac{dSOC'}{dSOC}$ can be calculated by Eq. (27):

$$\frac{dSOC'}{dSOC} = \frac{\left(\frac{1}{\delta} - 1\right) * \int Idt + \frac{1}{\delta} * \int I_s dt}{\int I_s dt}.$$
 (27)

Assuming I_s is also approximately constant, Eq. (27) can be simplified to the following:

$$\frac{dSOC'}{dSOC} = \frac{\left(\frac{1}{\delta} - 1\right) * I + \frac{1}{\delta} * I_s}{I_s}.$$
 (28)

Therefore, the capacity loss introduces the computational error expressed in Eq. (29):

$$\varepsilon = \left| \frac{\overline{V^{j}} / \left(dSOC * C_{0} \right) - \overline{V^{j}} / \left(dSOC * \delta * C_{0} \right)}{\overline{V} / \left(dSOC * C_{0} \right)} \right| * 100\%. \tag{29}$$

It can be simplified to the following equation:

$$\varepsilon = \left| 1 - 1 / \left(\frac{(1 - \delta) * I + I_s}{I_s} \right) \right| * 100\%$$
 (30)

For example, assuming the battery is discharging at a constant current of 10 A, with a short current of 0.04 A, and δ is 1.01, this will result in an estimated error of 71.7%.

4.2. Lab data analysis

Lab dataset, e.g., coin cell data, is cycle life based. Despite of hundreds of life cycles, directly quantifying the impact of soft ISC is challenging, as its effects on the battery are not evident in the short term and do not lead to significant degradation. Additionally, since short resistance is a highly sensitive indicator, its estimation is easily affected by factors such as capacity and k, leading to potential inaccuracies. As a result, we do not perform direct D&P algorithm evaluations on lab datasets. A more immediate reason is that we do not have the ground truth of short resistance in the lab datasets, only knowing that the cell is faulty without the ability to quantify it. Therefore, for lab datasets, we focus on evaluating indirect D&P algorithms, taking full advantage of the life cycle data to compare ISC D&P methods under different conditions, such as charging, discharging, and resting after charge/discharge. In our survey, we discuss many ISC diagnostic methods, each offering unique strengths in detecting internal short circuits in lithium-ion batteries. However, due to limitations such as the lack of available code and datasets, as well as the differing enabling conditions required by each method, it is challenging to evaluate and compare all these diagnostic techniques on a uniform dataset. To address this, we select 36 indirect diagnostic ISC D&P methods and evaluate them on the same dataset. This focused evaluation aims to provide a clearer understanding of the performance of these selected indicators under consistent conditions. In the following sections, we will discuss the results of this evaluation, highlighting key insights and their implications for ISC diagnostics.

We assess a set of 36 indicators across different laboratory data profiles to plot their True Positive Rate (TPR) against False Positive Rate (FPR). The assessment is designed to determine the efficacy of these indicators across all cycles and profiles, as well as their specificity to cycle lives or excitation conditions. 36 diagnostic methods listed in Table 1 are evaluated for fault isolation between soft faulty and healthy data. These diagnostic methods are categorized into nine distinct groups. The number preceding each ISC D&P method represents its corresponding index, which matches the numbers shown in Fig. 6.

To determine the effectiveness of a health indicator, a threshold that maximizes the distinction between healthy and faulty cells is required. The threshold is identified by evaluating the metric TPR+TNR, with the optimal threshold being the one that maximizes this value. Once the threshold is established, the corresponding TPR and FPR values under the test conditions are used to represent the indicator's performance, plotted as a dot in Fig. 6. The average TPR and FPR results for these 36 D&P methods over all available life cycles are presented in Fig. 6(a). Since some methods rely on dynamic charging/discharging data, and some methods only employ life cycle data, two different colors are used in Fig. 6. Purple dots represent the average values across approximately 10 cycles under dynamic charge/discharge conditions (Fig. 3 (c, e)), while blue dots indicate averages over 300 life cycles with constant charge and constant discharge conditions (Fig. 3(a)). The ISC D&P methods evaluated with selected life cycle data is presented in Fig. 6(b). Here, purple dots denote the values at the 5th cycle under dynamic charge/discharge conditions, while blue dots represent the values at the 100th cycle under constant charge and constant discharge conditions. Some common health indicators, such as Capacity (ISC D&P method 16) and Voltage drop (ISC D&P method 15), exhibit low TPRs, indicating limited effectiveness across the range of conditions. This suggests that these methods may not be effective to isolate ISC fault. Notably, the performance of ISC D&P methods when evaluated by specific life cycles (Fig. 6(b)) is superior to the average calculated across all cycles (Fig. 6(a)). This reflects that, even for the same health indicator, the threshold may vary across different life cycles as faults worsen and battery degradation progresses, resulting in substantial differences in dot distributions between Figs. 6 (a) and 6 (b).

Furthermore, the Voltage Slope after discharge (ISC D&P method 9) and Average Discharge Resistance (ISC D&P method 25) demonstrate outstanding performance by specific life cycle tests (Fig. 6(b)). By selecting and combining multiple health indicators, such as ISC D&P method 9 and 25, diagnostic accuracy could be enhanced. The fusion of these indicators allows for a tailored approach that accommodates the unique characteristics of each cell's life cycle and operational profile, thereby improving the overall diagnostic performance. These findings indicate the nuanced nature of battery health assessment and the importance of context in the application of ISC D&P methods. The potential to fine-tune diagnostics by cycle and profile conditions is a promising avenue for research.

4.3. Real vehicle data analysis

The real vehicle datasets are trip-based. Although the On-Vehicle Simulated ISC dataset is an exception as it does not include driving states, it does contain normal charging and low-current discharging states. The highly dynamic nature of trip-based data makes some indirect D&P algorithms (such as slope-based methods or methods based on charge/discharge energy differences within a cycle) unsuitable for evaluation on trip-based data. Additionally, for datasets like OnStar, which are from a large number of vehicles, there is no current or voltage signal. Unlike the lab datasets, the real vehicle datasets incorporate balancing mechanisms, which are rarely considered in indirect D&P algorithms. As a result, it is nearly impossible to directly apply D&P algorithms to these datasets. However, since real vehicle datasets include faulty cells, the evaluation of direct D&P algorithms is our focus.

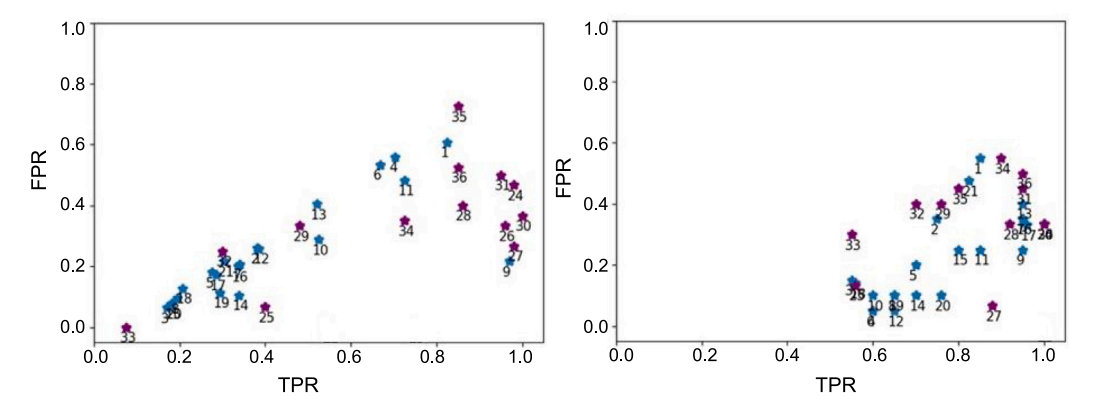


Fig. 6. Distribution of ISC D&P methods plotted as True Positive Rate (TPR) against False Positive Rate (FPR). Each point represents a distinct ISC D&P method. Blue points indicate the method evaluated with the 300-life-cycle dataset, while purple points indicate the method evaluated with the 10 cycles dataset, which requires dynamic current inputs. Indicators closer to the bottom-right corner of the plot demonstrate superior performance. (a) performance comparison with all available life cycle data. (For interpretation of the references to color in this figure legend, the reader is referred to the web version of this article.)

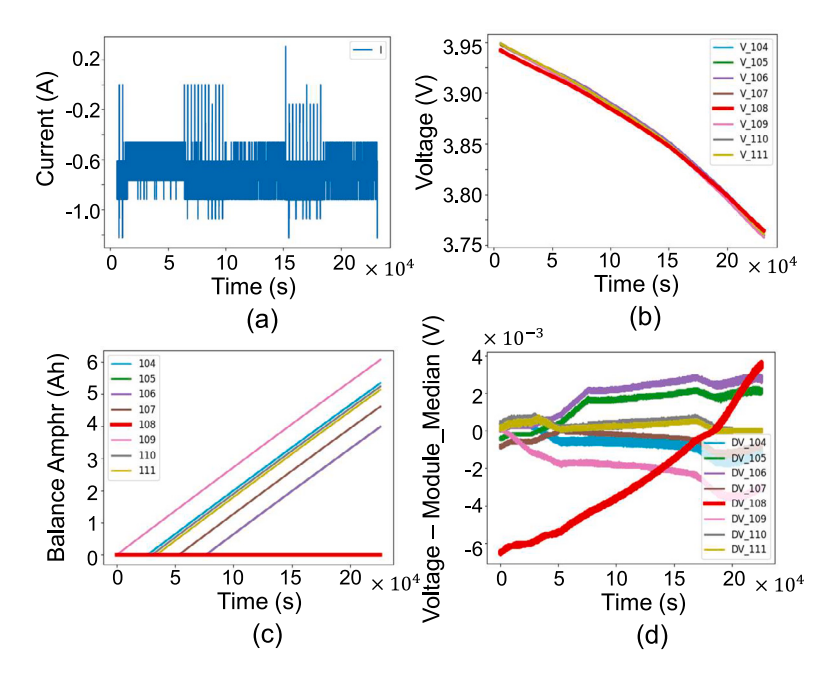


Fig. 7. A data segment from On-Vehicle Simulated ISC dataset. (a). Current signal of the pack; (b). Voltage signals of 8 cells from one module; (c). Balancing Amphr signals of 8 cells from the module. (d). Cell group voltage minus the module median voltage calculated from 8 cell groups from the module.

Fig. 7(a) shows a segment of the On-Vehicle Simulated ISC dataset during a discharge phase at -0.6 A, and Fig. 7(b) presents the voltage signal variation for one module under this discharge condition. It is observed that the voltage of the faulty cell (Cell 108) starts slightly lower than the other cells but, over time, the voltage difference gradually decreases. By the end, the voltage of this cell even slightly exceeds that of the other cells. Due to the balancing mechanism, as shown in Fig. 7(c), other cells reduce their voltage to maintain consistency in the OCV of the cells within the module. It is evident that the faulty cell does not participate in cell balancing during this process. To make this voltage change more apparent, the difference between the cell voltage and the module median (DV) is shown in Fig. 7(d). The DV curve clearly illustrates the differences between the faulty cell and the healthy cells, allowing for simple and accurate faulty cell isolation in this dataset.

Fig. 7 presents the DV curves for 192 cells from the On-Vehicle Simulated ISC dataset during a low-current discharge segment. The R_s values for Cells 108, 124, 140, 164 are selected at five discrete levels within the 500–1500 Ω range. It is evident that the more severe the ISC, indicated by a lower short resistance, leads to greater DV differences. From this figure, it can be observed that short resistance

can be roughly quantified through DV differences. However, to estimate short resistance, methods such as Cell Droop Rate is required, as they are derived from voltage-related differences caused by ISC. Table 5 lists the results of short resistance estimation using direct D&P methods. Since the dataset does not include SOC data, the estimation results of dSOC are not compared here. It is evident that there are significant deviations between the estimations and the ground truth values.

For Cell Droop Rate, short resistance estimation requires the current to be zero, making the method inapplicable in this case. To verify this understanding, considering the current is small, we apply this method directly. However, the estimated values for all cells are much smaller than the ground truth values, resulting in an estimated relative error of about 80% to 90%, since the current is significantly greater than the actual short circuit current. Therefore, existing direct D&P methods are not sufficiently accurate or robust for quantifying short resistance. One reason for this is the high sensitivity of short resistance estimation to external factors, making the enabling conditions of these methods more stringent. Additionally, errors introduced by sensors during signal acquisition cannot be overlooked. The significant estimation errors observed in Table 3 primarily result from current

Table 5
Performance evaluation on real vehicle data.

Method	CG108	CG124	CG140	CG164	CG188
Estimation error of Cell Droop Rate	79.87%	84.82%	88.31%	90.24%	92.11%

interference, sensor inaccuracies, and the stringent enabling conditions required by direct methods, such as zero-current scenarios for the Cell Droop Rate method. Improving robustness in dynamic environments necessitates advanced signal processing techniques for sensor data filtering, enhanced sensor accuracy, and incorporating adaptive calibration mechanisms. Additionally, the development of hybrid diagnostic models combining physics-based and data-driven techniques could further enhance the practical reliability of direct methods.

When comparing physics-based models and data-driven techniques, a comprehensive approach is adopted that considers their inherent characteristics and limitations. For physics-based models, model complexity, computational demands, and sensitivity to modeling parameters are explicitly assessed. In the case of data-driven methods, performance robustness is evaluated relative to data quality, quantity, and diversity. Specifically, sensitivity analysis is employed to quantify how variations in key parameters (such as the SOC mapping coefficient k and battery capacity C) influence estimation accuracy in physics-based methods. Meanwhile, data-driven techniques are evaluated based on their adaptability and performance across varying datasets, including real-world scenarios. Through such multi-dimensional evaluations, the comparative analysis offers clear and actionable insights into the most suitable application contexts for each diagnostic approach.

5. Challenges and future directions for ISC D&P

ISC D&P in lithium-ion batteries for EVs is crucial for improving EV driving experience. Current methods for detecting ISC are relatively effective and have been successfully integrated into production systems. However, achieving highly accurate ISC detection without triggering false positives or negatives remains a significant challenge.

Nonlinear, sudden, or near-hard shorts are difficult to model and capture early, as simplified models like ECMs lack the ability to represent detailed internal electrochemical processes. While physics-based P2D models offer higher accuracy, they are computationally intensive and unsuitable for real-time applications. This gap becomes critical when detecting intermittent shorts in pouch cells, where mechanical stress-induced deformation alters internal resistance within seconds. Moreover, accurate ISC detection depends heavily on sensor precision for voltage, current, and temperature, with sensor noise and reliability under harsh EV conditions often leading to false positives or missed detections.

The scarcity of high-quality, labeled data for ISC faults exacerbates these issues. Most public datasets lack controlled fault injection under realistic operating conditions, forcing researchers to rely on synthetic data that oversimplifies failure modes. This data paucity directly impacts diagnostic reliability—machine learning models trained on simulated dendrite growth patterns show lower accuracy when applied to real-world battery packs. Furthermore, the transient nature of mechanical stress-induced shorts creates detection blind spots. Pressure sensors embedded in pouch cells can detect swelling from gas generation, but their low sampling rates often miss sub-second mechanical relaxation events preceding ISC initiation.

Non-electrical sensing modalities introduce complementary challenges. Gas sensors (CO, $\rm H_2$) and ultrasonic probes provide post-failure confirmation rather than early warning. Thermal imaging achieves faster response but struggles to distinguish ISC-induced hotspots from normal temperature gradients during fast charging. Emerging techniques like distributed fiber optic sensing show promise in detecting localized strain variations but require fundamental redesigns of cell packaging.

Future research should focus on improving sensor technology, data availability, and modeling techniques. Enhancing sensor precision, along with the integration of multi-sensor fusion approaches, can improve ISC detection by combining voltage, current, thermal, and acoustic signals to provide a more comprehensive fault signature. Additionally, research into adaptive calibration methods for BMS sensors will be crucial in mitigating environmental noise and improving detection reliability. To address data scarcity, efforts should be directed toward developing standardized, large-scale datasets for ISC research. This includes leveraging synthetic data generation techniques, such as physics-informed machine learning, to create realistic ISC scenarios for training deep learning models. Furthermore, advanced diagnostic algorithms, such as Koopman mode analysis and hybrid model approaches, could enhance ISC detection accuracy [43]. By integrating the computational efficiency of ECMs with the physical accuracy of P2D models, these hybrid techniques offer a promising path toward realtime ISC detection in EV applications. In addition, refining machine learning-based classifiers to better correlate short resistance variations with specific failure modes will be essential in reducing false alarms. Future research should explore the coupling of electro-thermal models with real-time estimation frameworks, such as extended Kalman filters (EKF), which have shown promise in tracking ISC state evolution under dynamic conditions [121].

In addition, differentiating ISC-induced self-discharge from natural battery aging processes, such as SEI thickening and capacity fading, remains a critical challenge. To enhance the reliability of ISC detection, future research should explore integrating SOH estimation models with ISC diagnostics, leveraging collaborative diagnosis frameworks. Such integration would provide a clearer distinction between normal degradation and ISC-related faults, enabling more precise maintenance decisions and enhanced safety management.

A promising direction for future research is the integration of machine learning approaches with physics-based models, often termed hybrid modeling. Such integrated models leverage the computational efficiency and predictive accuracy of machine learning alongside the interpretability and fundamental insights offered by physics-based approaches. For instance, combining Electrochemical Impedance Spectroscopy (EIS)-based methods with deep learning techniques can enable precise early-stage ISC detection with improved scalability.

To address the scalability issues for larger battery systems, future research should focus on developing hierarchical or modular diagnostic approaches, where data-driven methods provide rapid anomaly detection across the entire battery pack, and physics-based models subsequently perform detailed analyses on localized suspicious cells. Such hybrid frameworks can significantly reduce computational burdens while maintaining high diagnostic accuracy, enabling practical, real-time implementation in large-scale EV battery management systems.

6. Conclusion

In this work, we have conducted a comprehensive review and comparison of various diagnostic and prognostic (D&P) methods for detecting ISC in lithium-ion batteries. The surveyed approaches are categorized into indirect and direct methods based on their data sources and detection mechanisms. Indirect methods, which infer ISC from observable electrical signals such as voltage deviations or SOC inconsistencies are widely implemented in real-world EV applications. However, these methods often struggle with quantifying ISC severity and are prone to false positives and false negatives due to operational variability and external noise factors. On the other hand, direct

methods, including impedance-based and resistance estimation techniques, offer a more precise quantification of ISC faults by directly characterizing electrical pathways affected by short circuits. Despite their improved accuracy, these methods still face challenges in realworld deployment, as existing models often exhibit significant errors in estimating short resistance, requiring further refinement for online applications. Our evaluation reveals that direct ISC diagnostic methods such as Cell Droop Rate exhibit significant estimation errors (approximately 80%-90%) in real vehicle data, highlighting the critical need for improved robustness and accuracy. A key takeaway from our review is that while indirect ISC D&P methods are currently the most feasible for onboard EV monitoring, they require further advancements to reduce false alarms and improve robustness across diverse operating conditions. Meanwhile, direct methods, particularly those leveraging EIS and deep learning, show promising potential in enhancing ISC detection accuracy and early warning capabilities. However, the practical implementation of these approaches remains constrained by measurement complexity and computational efficiency.

The insights from this comprehensive review and analysis have significant implications for industry stakeholders such as battery manufacturers and EV companies. By identifying and clearly outlining the strengths and limitations of various ISC diagnostic and prognostic methods, our findings assist stakeholders in selecting appropriate and reliable ISC detection technologies suited to their specific operational needs. Particularly, our comparative evaluations provide critical guidance on adopting robust D&P methods that minimize false positives and enhance early detection capabilities, thereby improving battery safety and reliability. These insights can directly inform safety standards and operational guidelines for battery management systems, contributing to enhanced vehicle safety, reduced warranty costs, and improved consumer trust.

CRediT authorship contribution statement

Yongtao Yao: Writing – original draft, Visualization, Software, Methodology, Investigation. Xinyu Du: Writing – review & editing, Methodology, Investigation, Conceptualization. Shengbing Jiang: Methodology, Investigation, Conceptualization. Rasoul Salehi: Methodology, Investigation, Conceptualization. Erik Huemiller: Data curation. Weisong Shi: Writing – review & editing, Supervision.

Declaration of Generative AI and AI-assisted technologies in the writing process

During the preparation of this work we used ChatGPT in order to improve readability and language of the work. The tool was used solely for language polishing, and all figures, tables, formulas, and the ideas presented in the manuscript are entirely original or derived from relevant references. After using this tool, we reviewed and edited the content as needed and take full responsibility for the content of the publication.

Declaration of competing interest

The authors declare that they have no known competing financial interests or personal relationships that could have appeared to influence the work reported in this paper.

Acknowledgments

This work was sponsored by General Motors (GM). The authors would like to thank Yilu Zhang and Sanjeev Naik for their tremendous support to this research. The authors would like to also thank the members of Energy and Propulsion Systems Research Lab and Vehicle Mechatronic Embedded Controls, General Motors for the discussion and suggestions.

Data availability

The data that has been used is confidential.

References

- Y. Wang, X. Zhang, K. Li, G. Zhao, Z. Chen, Perspectives and challenges for future Lithium-ion battery control and management. 2023.
- [2] IEA, Global EV outlook 2024, 2024, [Online]. Available: https://www.iea.org/reports/global-ev-outlook-2024. (Accessed 27 January 2025).
- [3] X. Wu, K. Song, X. Zhang, N. Hu, L. Li, W. Li, L. Zhang, H. Zhang, Safety issues in Lithium-ion batteries: materials and cell design, Front. Energy Res. 7 (2019) 65
- [4] D. Ren, X. Feng, L. Liu, H. Hsu, L. Lu, L. Wang, X. He, M. Ouyang, Investigating the relationship between internal short circuit and thermal runaway of Lithiumion batteries under thermal abuse condition, Energy Storage Mater. 34 (2021) 563–573.
- [5] S. Illikainen, Environmental Impacts of Lithium-Ion Batteries (B.S. thesis), 2022,S. Illikainen.
- [6] Y. Wang, J. Tian, Z. Sun, L. Wang, R. Xu, M. Li, Z. Chen, A comprehensive review of battery modeling and state estimation approaches for advanced battery management systems. Renew. Sustain. Energy Rev. 131 (2020) 110015.
- [7] S. Vashisht, D. Rakshit, S. Panchal, M. Fowler, R. Fraser, Experimental estimation of heat generating parameters for battery module using inverse prediction method, Int. Commun. Heat Mass Transfer 162 (2025) 108539.
- [8] Q. Liu, F. Liu, S. Liu, Y. Wang, S. Panchal, M. Fowler, R. Fraser, J. Yuan, J. Zhao, Improved performance of Li-ion battery thermal management system by ternary hybrid nanofluid, J. Energy Storage 109 (2025) 115234.
- [9] E. Yousefi, V. Talele, U. Morali, D. Mishra, D. Ramasamy, K. Kadirgama, H. Najafi, S. Kanthale, S. Panchal, Liquid immersion cooling with enhanced Al2O3 nanofluid for large-format prismatic battery pack: numerical and statistical investigation, J. Therm. Anal. Calorim. (2025) 1–19.
- [10] G. Zhang, X. Wei, X. Tang, J. Zhu, S. Chen, H. Dai, Internal short circuit mechanisms, experimental approaches and detection methods of Lithium-ion batteries for electric vehicles: A review, Renew. Sustain. Energy Rev. 141 (2021) 110790.
- [11] M.-K. Tran, A. Mevawalla, A. Aziz, S. Panchal, Y. Xie, M. Fowler, A review of Lithium-ion battery thermal runaway modeling and diagnosis approaches, Processes 10 (6) (2022) 1192.
- [12] A. Samanta, S. Chowdhuri, S.S. Williamson, Machine learning-based data-driven fault detection/diagnosis of Lithium-ion battery: A critical review, Electronics 10 (11) (2021) 1309.
- [13] M.M. Mariani, I. Machado, V. Magrelli, Y.K. Dwivedi, Artificial intelligence in innovation research: A systematic review, conceptual framework, and future research directions, Technovation 122 (2023) 102623.
- [14] D. Qiao, X. Wei, B. Jiang, W. Fan, X. Lai, Y. Zheng, H. Dai, Quantitative diagnosis of internal short circuit for Lithium-ion batteries using relaxation voltage, IEEE Trans. Ind. Electron. (2024).
- [15] D. Qiao, X. Wei, B. Jiang, W. Fan, H. Gong, X. Lai, Y. Zheng, H. Dai, Data-driven fault diagnosis of internal short circuit for series-connected battery packs using partial voltage curves, IEEE Trans. Ind. Inform. 20 (4) (2024) 6751–6761.
- [16] J. Hu, H. He, Z. Wei, Y. Li, Disturbance-immune and aging-robust internal short circuit diagnostic for Lithium-ion battery, IEEE Trans. Ind. Electron. 69 (2) (2021) 1988–1999.
- [17] R. Ma, Y. Deng, X. Wang, Simplified electrochemical model assisted detection of the early-stage internal short circuit through battery aging, J. Energy Storage 66 (2023) 107478.
- [18] A. Abaza, S. Ferrari, H.K. Wong, C. Lyness, A. Moore, J. Weaving, M. Blanco-Martin, R. Dashwood, R. Bhagat, Experimental study of internal and external short circuits of commercial automotive pouch Lithium-ion cells, J. Energy Storage 16 (2018) 211–217.
- [19] Q. Wang, B. Jiang, B. Li, Y. Yan, A critical review of thermal management models and solutions of Lithium-ion batteries for the development of pure electric vehicles, Renew. Sustain. Energy Rev. 64 (2016) 106–128.
- [20] Q. Wang, P. Ping, X. Zhao, G. Chu, J. Sun, C. Chen, Thermal runaway caused fire and explosion of Lithium-ion battery, J. Power Sources 208 (2012) 210–224.
- [21] B. Liu, Y. Jia, J. Li, S. Yin, C. Yuan, Z. Hu, L. Wang, Y. Li, J. Xu, Safety issues caused by internal short circuits in Lithium-ion batteries, J. Mater. Chem. A 6 (43) (2018) 21475–21484.
- [22] X. Zhang, E. Sahraei, K. Wang, Li-ion battery separators, mechanical integrity and failure mechanisms leading to soft and hard internal shorts, Sci. Rep. 6 (1) (2016) 32578.
- [23] S. Yang, W. Wang, C. Lin, W. Shen, Y. Li, Investigation of internal short circuits of Lithium-ion batteries under mechanical abusive conditions, Energies 12 (10) (2019) 1885.
- [24] D. Cao, W. Li, Y. Zhang, T. Ji, X. Zhao, E. Cakmak, J. Zhu, A. Adomkevicius, H. Zhu, Nondestructively visualizing and understanding" soft short" and Li creeping in all-solid-state Lithium-Metal batteries, 2023.

- [25] P. Albertus, S. Babinec, S. Litzelman, A. Newman, Status and challenges in enabling the lithium metal electrode for high-energy and low-cost rechargeable batteries, Nat. Energy 3 (1) (2018) 16–21.
- [26] K. Xu, Electrolytes and interphases in Li-ion batteries and beyond, Chem. Rev. 114 (23) (2014) 11503–11618.
- [27] W. Gao, X. Li, M. Ma, Y. Fu, J. Jiang, C. Mi, Case study of an electric vehicle battery thermal runaway and online internal short-circuit detection, IEEE Trans. Power Electron. 36 (3) (2020) 2452–2455.
- [28] Y. Chen, L. Gao, R. Yang, Z. Wu, L. Zhang, Internal short circuit detection in battery pack based on internal resistance parameters, in: 2024 IEEE Transportation Electrification Conference and Expo, Asia-Pacific, ITEC Asia-Pacific, IEEE, 2024, pp. 1053–1058.
- [29] D. Aurbach, E. Zinigrad, Y. Cohen, H. Teller, A short review of failure mechanisms of lithium metal and lithiated graphite anodes in liquid electrolyte solutions, Solid State Ion. 148 (3–4) (2002) 405–416.
- [30] S.S. Zhang, A review on the separators of liquid electrolyte Li-ion batteries, J. Power Sources 164 (1) (2007) 351–364.
- [31] G.L. Plett, Extended Kalman filtering for battery management systems of LiPB-based HEV battery packs: Part 3. State and parameter estimation, J. Power Sources 134 (2) (2004) 277–292.
- [32] D. Andre, M. Meiler, K. Steiner, C. Wimmer, T. Soczka-Guth, D. Sauer, Characterization of high-power Lithium-ion batteries by electrochemical impedance spectroscopy. I. Experimental investigation, J. Power Sources 196 (12) (2011) 5334-5341
- [33] J.B. Goodenough, K.-S. Park, The Li-ion rechargeable battery: a perspective, J. Am. Chem. Soc. 135 (4) (2013) 1167–1176.
- [34] W. Xu, J. Wang, F. Ding, X. Chen, E. Nasybulin, Y. Zhang, J.-G. Zhang, Lithium metal anodes for rechargeable batteries, Energy Environ. Sci. 7 (2) (2014) 513–537
- [35] D.P. Finegan, M. Scheel, J.B. Robinson, B. Tjaden, I. Hunt, T.J. Mason, J. Millichamp, M. Di Michiel, G.J. Offer, G. Hinds, D.J. Brett, P.R. Shearing, In-operando high-speed tomography of Lithium-ion batteries during thermal runaway, Nat. Commun. 6 (1) (2015) 6924.
- [36] J. Christensen, J. Newman, A mathematical model of stress generation and fracture in lithium manganese oxide, J. Electrochem. Soc. 153 (6) (2006) A1019.
- [37] J. Manzi, F.M. Vitucci, A. Paolone, F. Trequattrini, D. Di Lecce, S. Panero, S. Brutti, Analysis of the self-discharge process in LiCoPO4 electrodes: bulks, Electrochim. Acta 179 (2015) 604–610.
- [38] M. Petzl, M. Kasper, M.A. Danzer, Lithium plating in a commercial Lithium-ion battery–A low-temperature aging study, J. Power Sources 275 (2015) 799–807.
- [39] X. Feng, M. Ouyang, X. Liu, L. Lu, Y. Xia, X. He, Thermal runaway mechanism of Lithium-ion battery for electric vehicles: A review, Energy Storage Mater. 10 (2018) 246–267.
- [40] R. Spotnitz, Simulation of capacity fade in Lithium-ion batteries, J. Power Sources 113 (1) (2003) 72–80.
- [41] L. Gaines, The future of automotive Lithium-ion battery recycling: Charting a sustainable course, Sustain. Mater. Technol. 1 (2014) 2–7.
- [42] P. Sun, R. Bisschop, H. Niu, X. Huang, A review of battery fires in electric vehicles, Fire Technol. 56 (4) (2020) 1361–1410.
- [43] S. Ghosh, S. Mallick, T. Roy, Koopman mode-based detection of internal short circuits in Lithium-ion battery pack, 2024, arXiv preprint arXiv:2412.13115.
- [44] X. Lai, C. Jin, W. Yi, X. Han, X. Feng, Y. Zheng, M. Ouyang, Mechanism, modeling, detection, and prevention of the internal short circuit in Lithium-ion batteries: Recent advances and perspectives, Energy Storage Mater. 35 (2021) 470–499.
- [45] Q.-K. Wang, Y.-J. He, J.-N. Shen, X.-S. Hu, Z.-F. Ma, State of charge-dependent polynomial equivalent circuit modeling for electrochemical impedance spectroscopy of Lithium-ion batteries, IEEE Trans. Power Electron. 33 (10) (2017) 8449–8460
- [46] M. Furugori, N. Katayama, Automated determination of equivalent circuit models for electrochemical systems using EIS and machine learning, in: 2024 13th International Conference on Renewable Energy Research and Applications, ICRERA, IEEE, 2024, pp. 699–704.
- [47] M. Safari, C. Delacourt, Modeling of a commercial graphite/LiFePO4 cell, J. Electrochem. Soc. 158 (5) (2011) A562.
- [48] A. Melcher, C. Ziebert, M. Rohde, B. Lei, H.J. Seifert, ECM Models for Li-Ion Batteries-A Short Mathematical Survey and Simulations, KIT Scientific Publishing, 2018.
- [49] X. Liu, Z. Zhou, W. Wu, L. Gao, Y. Li, H. Huang, Z. Huang, Y. Li, Y. Song, Three-dimensional modeling for the internal shorting caused thermal runaway process in 20AH Lithium-ion battery, Energies 15 (19) (2022) 6868.
- [50] Y. Jia, L. Brancato, M. Giglio, F. Cadini, Enhancing lithium-ion battery safety: Analysis and detection of internal short circuit basing on an electrochemical-thermal modeling, in: PHM Society European Conference, vol. 8, (1) 2024, 7–7
- [51] Z. Chen, X. Xiao, Y. Wang, L. Li, S. Wei, Numerical simulation model construction for ISC faults in Lithium-ion battery, in: 2023 8th International Conference on Power and Renewable Energy, ICPRE, IEEE, 2023, pp. 220–226.

- [52] J. Zhou, B. Xing, C. Wang, A review of Lithium-ion batteries electrochemical models for electric vehicles, in: E3S Web of Conferences, vol. 185, EDP Sciences, 2020, p. 04001.
- [53] Q. Yao, P. Kollmeyer, J. Chen, S. Panchal, O. Gross, A. Emadi, Study of High-Power and High-Energy Lithium-ion Batteries: From Parameter Analysis to Physical Modeling and Experimental Validation, Tech. Rep., SAE Technical Paper. 2025.
- [54] A. Fotouhi, D.J. Auger, K. Propp, S. Longo, M. Wild, A review on electric vehicle battery modelling: From Lithium-ion toward Lithium-Sulphur, Renew. Sustain. Energy Rev. 56 (2016) 1008–1021.
- [55] H. Li, B. Liu, D. Zhou, C. Zhang, Coupled mechanical-electrochemical-thermal study on the short-circuit mechanism of Lithium-ion batteries under mechanical abuse, J. Electrochem. Soc. 167 (12) (2020) 120501.
- [56] J. Deng, C. Bae, J. Marcicki, A. Masias, T. Miller, Safety modelling and testing of Lithium-ion batteries in electrified vehicles, Nat. Energy 3 (4) (2018) 261–266.
- [57] L. Wang, J. Li, J. Chen, X. Duan, B. Li, J. Li, Revealing the internal short circuit mechanisms in Lithium-ion batteries upon dynamic loading based on multiphysics simulation, Appl. Energy 351 (2023) 121790.
- [58] H. Li, D. Zhou, M. Zhang, B. Liu, C. Zhang, Multi-field interpretation of internal short circuit and thermal runaway behavior for Lithium-ion batteries under mechanical abuse, Energy 263 (2023) 126027.
- [59] B. Xia, Y. Shang, T. Nguyen, C. Mi, A correlation based fault detection method for short circuits in battery packs, J. Power Sources 337 (2017) 1–10.
- [60] X. Feng, Y. Pan, X. He, L. Wang, M. Ouyang, Detecting the internal short circuit in large-format Lithium-ion battery using model-based fault-diagnosis algorithm, J. Energy Storage 18 (2018) 26–39.
- [61] Z. Sun, Z. Wang, Y. Chen, P. Liu, S. Wang, Z. Zhang, D.G. Dorrell, Modified relative entropy-based Lithium-ion battery pack online short-circuit detection for electric vehicle, IEEE Trans. Transp. Electrification 8 (2) (2021) 1710–1723.
- [62] G. Wang, J. Zhao, J. Yang, J. Jiao, J. Xie, F. Feng, Multivariate statistical analysis based cross voltage correlation method for internal short-circuit and sensor faults diagnosis of Lithium-ion battery system, J. Energy Storage 62 (2023) 106978.
- [63] A.A. Pesaran, C. Yang, NREL Multiphysics Modeling Tools and ISC Device for Designing Safer Li-Ion Batteries, Tech. Rep., National Renewable Energy Lab.(NREL), Golden, CO (United States), 2016.
- [64] Y. Chen, NASA lithium ion battery dataset, 2024, [Online]. Available: https://ieee-dataport.org/documents/nasa-lithium-ion-battery-dataset.
- [65] Randomized battery usage 1: Random walk, 2025, https://data.nasa.gov/ Raw-Data/Randomized-Battery-Usage-1-Random-Walk/ugxu-9kjx. (Accessed 18 January 2025).
- [66] C. Birkl, Diagnosis and Prognosis of Degradation in Lithium-Ion Batteries (Ph.D. thesis), University of Oxford, 2017.
- [67] M. Steinstraeter, J. Buberger, D. Trifonov, Battery and heating data in real driving cycles, IEEE Dataport 10 (2020).
- [68] M. Pecht, Battery data, 2025, https://calce.umd.edu/battery-data. (Accessed 18 January 2025).
- [69] W. Chen, J. Jiang, J. Wen, Thermal runaway induced by dynamic overcharge of Lithium-ion batteries under different environmental conditions, J. Therm. Anal. Calorim. 146 (2) (2021) 855–863.
- [70] S.V. Sazhin, E.J. Dufek, K.L. Gering, Enhancing Li-ion battery safety by early detection of nascent internal shorts, Ecs Trans. 73 (1) (2016) 161.
- [71] Z. Sun, Z. Wang, P. Liu, Z. Qin, Y. Chen, Y. Han, P. Wang, P. Bauer, An online data-driven fault diagnosis and thermal runaway early warning for electric vehicle batteries, IEEE Trans. Power Electron. 37 (10) (2022) 12636–12646.
- [72] B. Cui, H. Wang, R. Li, L. Xiang, J. Du, H. Zhao, S. Li, X. Zhao, G. Yin, X. Cheng, Y. Ma, H. Huo, P. Zuo, C. Du, Internal short circuit early detection of Lithium-ion batteries from impedance spectroscopy using deep learning, J. Power Sources 563 (2023) 232824.
- [73] M. Dotoli, R. Rocca, M. Giuliano, G. Nicol, F. Parussa, M. Baricco, A.M. Ferrari, C. Nervi, M.F. Sgroi, A review of mechanical and chemical sensors for automotive Li-ion battery systems, Sensors 22 (5) (2022) 1763.
- [74] J. Xu, J. Ma, X. Zhao, H. Chen, B. Xu, X. Wu, Detection technology for battery safety in electric vehicles: A review, Energies 13 (18) (2020) 4636.
- [75] L. Zhou, L. Xing, Y. Zheng, X. Lai, J. Su, C. Deng, T. Sun, A study of external surface pressure effects on the properties for Lithium-ion pouch cells, Int. J. Energy Res. 44 (8) (2020) 6778–6791.
- [76] R. Ma, J. He, Y. Deng, Investigation and comparison of the electrochemical impedance spectroscopy and internal resistance indicators for early-stage internal short circuit detection through battery aging, J. Energy Storage 54 (2022) 105346.
- [77] Y. Zhang, P. Zhang, J. Hu, C. Zhang, L. Zhang, Y. Wang, W. Zhang, Fault diagnosis method of Lithium-ion battery leakage based on electrochemical impedance spectroscopy, IEEE Trans. Ind. Appl. (2023).
- [78] M. Koseoglou, E. Tsioumas, D. Papagiannis, N. Jabbour, C. Mademlis, A novel on-board electrochemical impedance spectroscopy system for real-time battery impedance estimation, IEEE Trans. Power Electron. 36 (9) (2021) 10776–10787.
- [79] L.A. Middlemiss, A.J. Rennie, R. Sayers, A.R. West, Characterisation of batteries by electrochemical impedance spectroscopy, Energy Rep. 6 (2020) 232–241.

- [80] I. Ezpeleta, L. Freire, C. Mateo-Mateo, X.R. Nóvoa, A. Pintos, S. Valverde-Pérez, Characterisation of commercial Li-ion batteries using electrochemical impedance spectroscopy, ChemistrySelect 7 (10) (2022) e202104464.
- [81] J. Chen, P. Kollmeyer, S. Panchal, Y. Masoudi, Techniques for measuring battery system state of power, 2025, US Patent App. 18/362, 385.
- [82] A. Naha, A. Khandelwal, S. Agarwal, P. Tagade, K.S. Hariharan, A. Kaushik, A. Yadu, S.M. Kolake, S. Han, B. Oh, Internal short circuit detection in Li-ion batteries using supervised machine learning, Sci. Rep. 10 (1) (2020) 1301.
- [83] H. Liu, S. Hao, T. Han, F. Zhou, G. Li, Random forest-based online detection and location of internal short circuits in lithium battery energy storage systems with limited number of sensors, IEEE Trans. Instrum. Meas. (2023).
- [84] X. Wu, Z. Wei, T. Wen, J. Du, J. Sun, A. Shtang, Research on short-circuit fault-diagnosis strategy of Lithium-ion battery in an energy-storage system based on voltage cosine similarity, J. Energy Storage 71 (2023) 108012.
- [85] M. Schmid, J. Kleiner, C. Endisch, Early detection of internal short circuits in series-connected battery packs based on nonlinear process monitoring, J. Energy Storage 48 (2022) 103732.
- [86] X. Li, Z. Wang, A novel fault diagnosis method for Lithium-ion battery packs of electric vehicles, Measurement 116 (2018) 402–411.
- [87] L. Brancato, Y. Jia, M. Giglio, F. Cadini, Prognosis of internal short circuit formation in Lithium-Ion batteries: An integrated approach using extended Kalman filter and regression model, in: PHM Society European Conference, vol. 8. (1) 2024. 8–8.
- [88] S. Zhao, Q. Peng, J. Fang, K. Li, L. Ye, K. Liu, Internal short-circuit diagnosis method in Lithium-Ion battery based on temporal convolutional network voltage prediction, in: International Conference on Life System Modeling and Simulation, Springer, 2024, pp. 244–253.
- [89] R.F. De Mello, M.A. Ponti, Statistical learning theory, Mach. Learn. 3 (2018).
- [90] J. Cervantes, F. Garcia-Lamont, L. Rodríguez-Mazahua, A. Lopez, A comprehensive survey on support vector machine classification: Applications, challenges and trends, Neurocomputing 408 (2020) 189–215.
- [91] L. Yao, Z. Fang, Y. Xiao, J. Hou, Z. Fu, An intelligent fault diagnosis method for lithium battery systems based on grid search support vector machine, Energy 214 (2021) 118866.
- [92] N. Gan, Z. Sun, Z. Zhang, S. Xu, P. Liu, Z. Qin, Data-driven fault diagnosis of Lithium-ion battery overdischarge in electric vehicles, IEEE Trans. Power Electron. 37 (4) (2021) 4575–4588.
- [93] L. Breiman, Random forests, Mach. Learn. 45 (2001) 5-32.
- [94] Y. Jia, J. Li, W. Yao, Y. Li, J. Xu, Precise and fast safety risk classification of Lithium-ion batteries based on machine learning methodology, J. Power Sources 548 (2022) 232064.
- [95] F. Noori, M. Moeini-Aghtaie, Enhanced internal short circuit diagnosis of lithium-ion batteries using an equivalent circuit model and machine learning algorithms, in: 2024 9th International Conference on Technology and Energy Management, ICTEM, IEEE, 2024, pp. 1–6.
- [96] S. Vassilvitskii, D. Arthur, k-means++: The advantages of careful seeding, in: Proceedings of the Eighteenth Annual ACM-SIAM Symposium on Discrete Algorithms, 2006, pp. 1027–1035.
- [97] M. Wu, W. Du, F. Zhang, N. Zhao, J. Wang, L. Wang, W. Huang, Fault diagnosis method for Lithium-ion battery packs in real-world electric vehicles based on K-means and the Fréchet algorithm. ACS Omega 7 (44) (2022) 40145–40162.
- [98] Q. Liu, J. Ma, X. Zhao, K. Zhang, D. Meng, Online diagnosis and prediction of power battery voltage comprehensive faults for electric vehicles based on multi-parameter characterization and improved K-means method, Energy 283 (2023) 129130.
- [99] K. Pearson, VII. Note on regression and inheritance in the case of two parents, Proc. R. Soc. Lond. 58 (347–352) (1895) 240–242.

- [100] G. Wang, S. Jin, G. Zhao, J. Zhao, J. Xie, An independent component analysis based correlation coefficient method for internal short-circuit fault diagnosis of battery-powered intelligent transportation systems, Control Eng. Pract. 138 (2023) 105506.
- [101] Z.-H. Zhou, Ensemble Methods: Foundations and Algorithms, CRC Press, 2025.
- [102] Y. Freund, R.E. Schapire, A decision-theoretic generalization of on-line learning and an application to boosting, J. Comput. System Sci. 55 (1) (1997) 119–139.
- [103] G. Wang, G. Zhao, J. Xie, K. Liu, Ensemble learning-based correlation coefficient method for robust diagnosis of voltage sensor and short-circuit faults in series battery packs, IEEE Trans. Power Electron. 38 (7) (2023) 9143–9156.
- [104] Y. Jia, J. Xu, Data-driven short circuit resistance estimation in battery safety issues, J. Energy Chem. 79 (2023) 37–44.
- [105] J. Schmidhuber, Deep learning in neural networks: An overview, Neural Netw. 61 (2015) 85–117.
- [106] R. Yang, R. Xiong, S. Ma, X. Lin, Characterization of external short circuit faults in electric vehicle Li-ion battery packs and prediction using artificial neural networks, Appl. Energy 260 (2020) 114253.
- [107] Y. LeCun, Y. Bengio, G. Hinton, Deep learning, Nature 521 (7553) (2015) 436–444.
- [108] G. Zhu, T. Sun, Y. Xu, Y. Zheng, L. Zhou, Identification of internal short-circuit faults in Lithium-ion batteries based on a multi-machine learning fusion, Batteries 9 (3) (2023) 154.
- [109] H. Liu, T. Han, S. Hao, G. Li, Internal short circuit fault diagnosis based on 1DVCNN in lithium battery storage system, Energy Rep. 9 (2023) 1470–1479.
- [110] Y. Liu, C. Liao, W. Zhang, G. Hu, C. Zhang, L. Wang, Internal short circuit diagnosis of Lithium-ion battery based on mechanism model and deep learning, J. Electrochem. Soc. 169 (10) (2022) 100514.
- [111] N. Yang, Z. Song, M.R. Amini, H. Hofmann, Internal short circuit detection for parallel-connected battery cells using convolutional neural network, Automot. Innov. 5 (2) (2022) 107–120.
- [112] M. Seo, T. Goh, M. Park, S.W. Kim, Detection of internal short circuit for Lithium-ion battery using convolutional neural networks with data pre-processing, Int. J. Electron. Electr. Eng. (2019) 6–11.
- [113] D. Krotov, J.J. Hopfield, Dense associative memory for pattern recognition, Adv. Neural Inf. Process. Syst. 29 (2016).
- [114] A. Graves, A. Graves, "Long Short-Term Memory," Supervised Sequence Labelling with Recurrent Neural Networks, Springer, 2012, pp. 37–45.
- [115] N. Wang, Q. Yang, J. Xing, H. Jia, W. Chen, Thermal fault diagnosis method of Lithium battery based on LSTM and battery physical model, in: 2022 41st Chinese Control Conference, CCC, IEEE, 2022, pp. 4147–4152.
- [116] A. Vaswani, N. Shazeer, N. Parmar, J. Uszkoreit, L. Jones, A.N. Gomez, L. Kaiser, I. Polosukhin, Attention is all you need, in: Proceedings of the 31st International Conference on Neural Information Processing Systems, NIPS '17, Curran Associates Inc., Red Hook, NY, USA, 2017, pp. 6000–6010.
- [117] H. Wang, J. Nie, Z. He, M. Gao, W. Song, Z. Dong, A reconstruction-based model with transformer and long short-term memory for internal short circuit detection in battery packs, Energy Rep. 9 (2023) 2420–2430.
- [118] Z. Dong, S. Gu, S. Zhou, M. Yang, C.S. Lai, M. Gao, X. Ji, Periodic segmentation transformer-based internal short circuit detection method for battery packs, IEEE Trans. Transp. Electrification (2024).
- [119] Y.-Y. Wang, Y. Zeng, T.R. Garrick, A.C. Baughman, Method and system for self-discharge prognostics for vehicle battery cells with an internal short circuit, 2023, US Patent number: US 11, 733, 309 B2.
- [120] Y.-Y. Wang, A.C. Baughman, Thermal runaway prognosis by detecting abnormal cell voltage and soc degeneration, 2022, US Patent Publication Number: US 20220352737A1.
- [121] Y. Jia, L. Brancato, F. Cadini, M. Giglio, Real-time detection of internal short circuits in Lithium-ion batteries using an extend Kalman filter: A novel approach combining electrical and thermal measurements, Int. J. Progn. Heal. Manag. 15 (3) (2024).